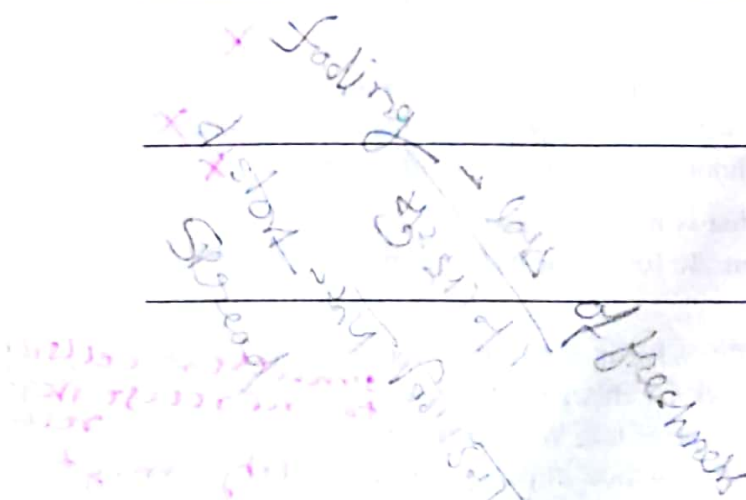


# 2

## Characterization of the Wireless Channel



Impairments in the propagation channel have the effect of disturbing the information carried by the transmitted signal. Channel disturbance can be a combination of additive noise, multiplicative fading, and distortion due to time dispersion. The focus of this chapter is to characterize the wireless channel by identifying the parameters of the corruptive elements that distort the information-carrying signal as it penetrates the propagation medium. The corruptive elements are in the form of multipath delay spread, Doppler spread due to motion, and signal fading of the frequency-selective and non-frequency-selective variety. The propagation channel is normally time-variant. In this chapter, we first model the channel as linear time-variant, and then characterize Doppler spread, multipath delay spread, and fading in terms of second order statistics.

### 2.1 MULTIPATH PROPAGATION ENVIRONMENT

The wireless propagation channel contains objects (particles) which randomly scatter the energy of the transmitted signal. The scattered signals arrive at the destination receiver out of step. These objects (particles) are referred to as scatterers. Scatterers introduce a variety of channel impairments including fading, multipath delay spread, Doppler spread, attenuation, etc., and the inherent background noise. Background noise can be approximated as thermal noise and treated as additive white Gaussian noise (AWGN). Digital transmission over practical wireless channels is mainly limited by interference and distortion other than AWGN.

Scattering by randomly located scatterers gives rise to different paths with different path lengths, resulting in multipath delay spread. Consider a point source (a single tone sinusoid) as a test signal. If the propagation channel does not exhibit multipath delay spread, the point source would appear at the front end of the receiver as another point source. A multipath situation arises when a transmitted point source is received as a multipoint source, with each of the individually received points experiencing a different transmission delay. A pictorial view of the scattering phenomenon is depicted in Figure 2.1. The effect of multipath propagation on digital transmission can be characterized by time dispersion and fading.

**Time Dispersion.** Because multiple propagation paths have different propagation delays, the transmitted point source will be received as a smeared waveform. Nonoverlapping scatterers give rise to distinct multiple paths, which are characterized by their locations in the scattering medium. As depicted in Figure 2.2, all scatterers are located on ellipses with the transmitter (Tx) and receiver (Rx) as the foci. One ellipse is associated with one path length. Therefore, signals reflected by scatterers located on the same ellipse will experience the same propagation delay. The signal components from these multiple paths are indistinguishable at the receiver. Signals that are reflected by scatterers located on different ellipses will arrive at the receiver with differential

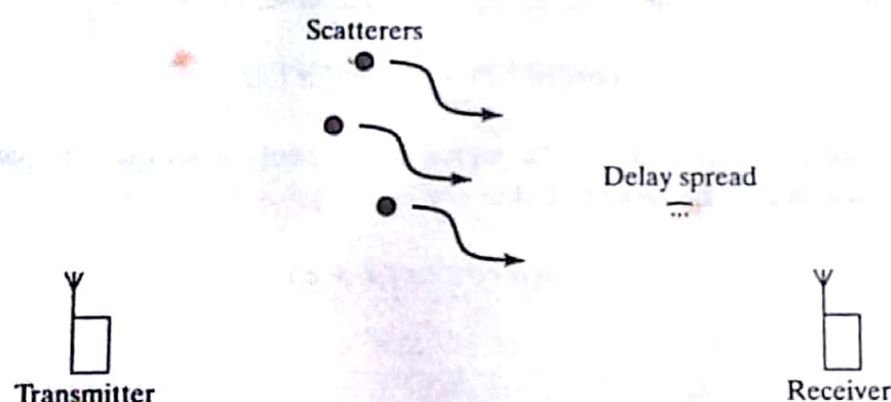


Figure 2.1 Multipath spread due to channel scattering.

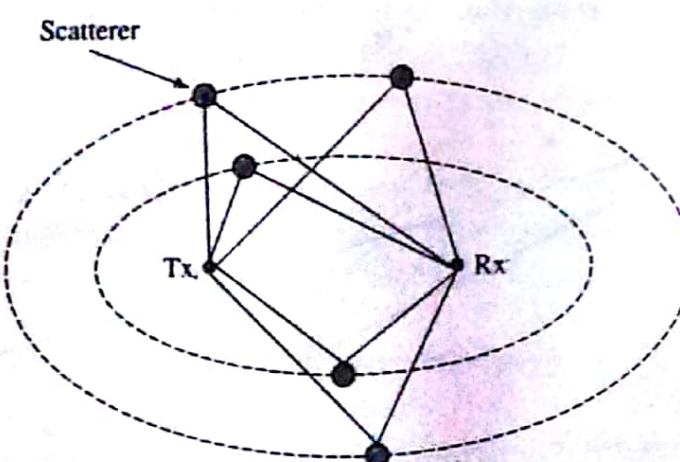


Figure 2.2 Ellipsoidal portrayal of scatterer location.

delays. If the maximum differential delay spread is small compared with the symbol duration of the transmitted signal, the channel is said to exhibit flat fading. If the differential delay spread is large compared with the symbol interval, the channel exhibits frequency-selective fading. In the time domain, the received signals corresponding to successive transmitted symbols will overlap, giving rise to a phenomenon known as intersymbol interference (ISI). ISI is a signal-dependent distortion. The severity of ISI increases with the width of the delay spread. The ISI distortion in the time domain can also be examined in the frequency domain. ISI degrades transmission performance. Channel equalization techniques can be used to combat ISI, as discussed in Chapter 4.

**Fading.** When the delay differences among various distinct propagation paths are very small compared with the symbol interval in digital transmission, the multipath components are almost indistinguishable at the receiver. These multipath components can add constructively or destructively, depending on the carrier frequency and delay differences. In addition, as the mobile station moves, the position of each scatterer with respect to the transmitter and receiver may change. The overall effect is that the received signal level fluctuates with time, a phenomenon called fading. As an example, consider the transmission of a single-tone sinusoidal signal with frequency  $f_c$  over a channel with two distinct paths, as shown in Figure 2.3. For simplicity, the delay of the line-of-sight (LOS) or direct path is assumed to be zero, and the delay of the non-line-of-sight (NLOS) or reflected path is  $\tau$ . The received signal, in the absence of noise, can be represented as

$$r(t) = \alpha_1 \cos(2\pi f_c t) + \alpha_2 \cos(2\pi f_c(t - \tau)), \quad (2.1.1)$$

where  $\alpha_1$  and  $\alpha_2$  are the amplitudes of the signal components from the two paths respectively. The received signal can also be represented as

$$r(t) = \alpha \cos(2\pi f_c t + \phi), \quad (2.1.2)$$

where

$$\alpha = \sqrt{\alpha_1^2 + \alpha_2^2 + 2\alpha_1\alpha_2 \cos(2\pi f_c \tau)}$$

and

$$\phi = -\tan^{-1} \left[ \frac{\alpha_2 \sin(2\pi f_c \tau)}{\alpha_1 + \alpha_2 \cos(2\pi f_c \tau)} \right]$$

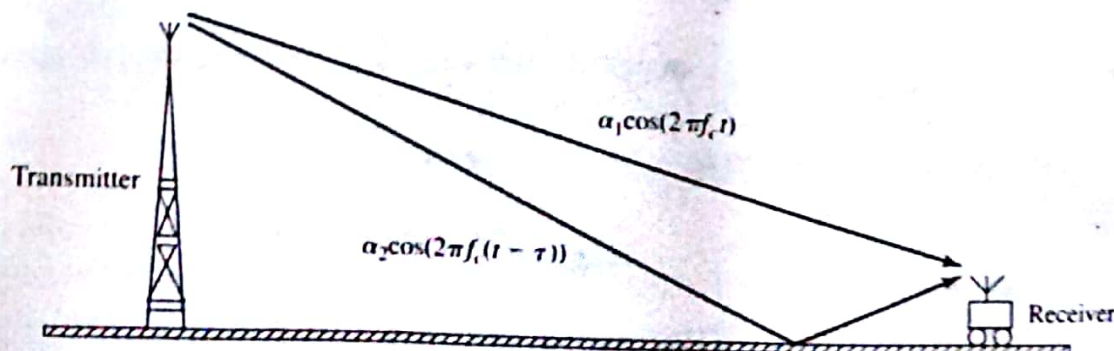


Figure 2.3 A channel with two propagation paths.

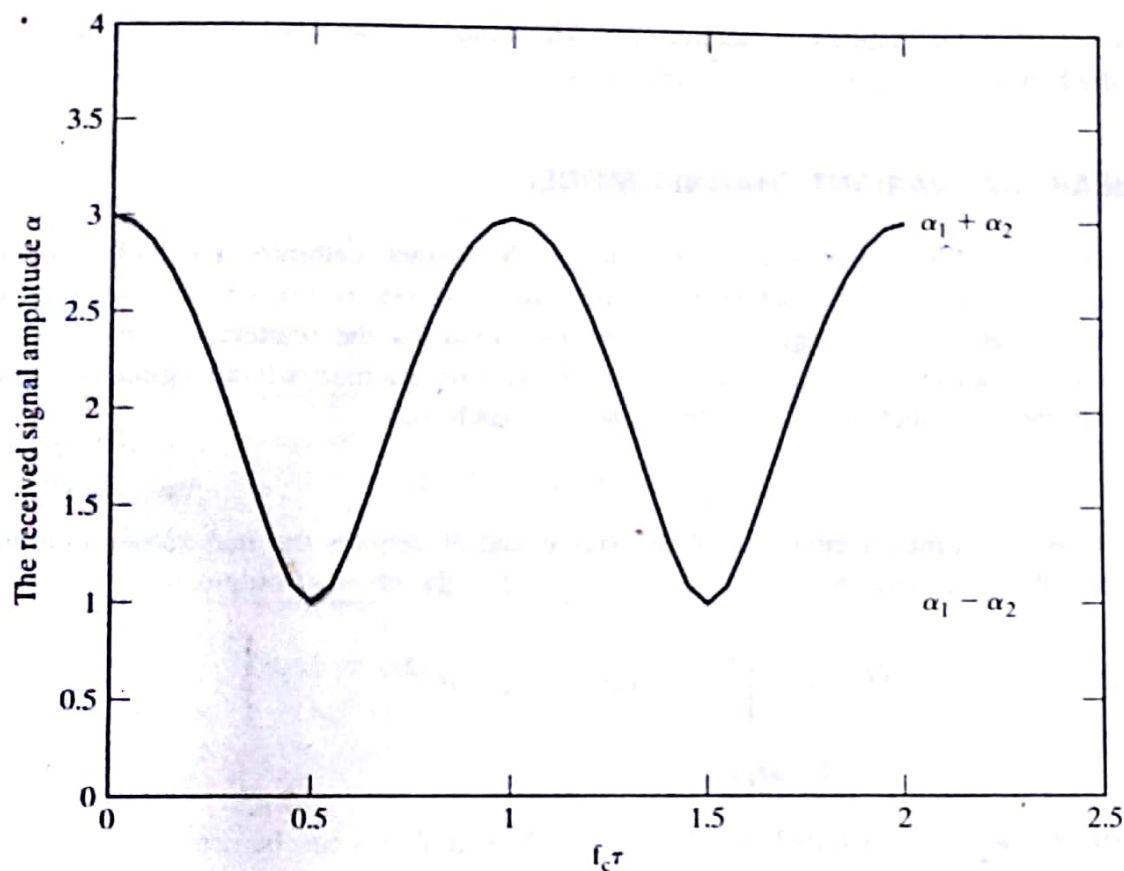


Figure 2.4 The amplitude fluctuation of the two-path channel with  $\alpha_1 = 2$  and  $\alpha_2 = 1$ .

are the amplitude and phase of the received signal. Both  $\alpha$  and  $\phi$  are functions of  $\alpha_1$ ,  $\alpha_2$ , and  $\tau$ . Figure 2.4 plots the amplitude  $\alpha$  as a function of  $f_c\tau$ , where  $\alpha_1 = 2$  and  $\alpha_2 = 1$ . It can be observed that the two received signal components add constructively when  $f_c\tau = 0, 1, 2, \dots$  and destructively when  $f_c\tau = 0.5, 1.5, 2.5, \dots$ . In general, as the mobile station moves,  $\alpha_1$ ,  $\alpha_2$ , and  $\tau$  change with time. The received signal amplitude  $\alpha$  and phase  $\phi$  also change with time. When the signal components from the two paths add destructively, the transmitted signal experiences deep fading with a small value of the amplitude  $\alpha$ . During each deep fade, the instantaneously received signal power is very low, resulting in poor transmission quality (i.e., high transmission error rate). Diversity and error-correction coding (with interleaving) are effective to combat channel fading for better transmission accuracy, as discussed in Chapter 4.

The channel fading can be classified as long-term fading or short-term fading. The former is a large-scale path-loss, characterizing the local average of the path loss, as discussed in Section 2.4. The latter describes the instantaneously received signal level variations with respect to the local average, as discussed in Section 2.5.

In summary, multipath propagation in the wireless mobile environment results in a fading dispersive channel. The signal propagation environment changes as the mobile station moves and/or as any surrounding scatterers move. Therefore, the channel is time varying and can be modeled as a linear time-variant (LTV) system. In the following sections, we first study how to describe a wireless channel using the LTV model in Section 2.2, and then focus on the correlation

functions of the LTV channel in Section 2.3. The long-term and short-term fading models are then studied in Sections 2.4 and 2.5 respectively.

## 2.2 LINEAR TIME-VARIANT CHANNEL MODEL

Consider a multipath propagation environment with  $N$  distinct scatterers. The path associated with the  $n$ th distinct scatterer is characterized by the 2-tuple  $(\alpha_n(t), \tau_n(t))$ , where  $\alpha_n(t)$  represents the amplitude fluctuation introduced to the transmitted signal by the scatterer at time  $t$ ,  $\tau_n(t)$  is the associated propagation delay, and  $n = 1, 2, \dots, N$ . Consider a narrowband signal  $\tilde{x}(t)$  transmitted over the wireless channel at a carrier frequency  $f_c$ , such that

$$\tilde{x}(t) = \Re\{x(t)e^{j2\pi f_c t}\}, \quad (2.2.1)$$

where  $x(t)$  is the complex envelope of the signal and  $\Re$  denotes the real-valued component. In the absence of background noise, the received signal at the channel output is

$$\begin{aligned} \tilde{r}(t) &= \Re \left\{ \sum_{n=1}^N \alpha_n(t) x(t - \tau_n(t)) e^{j2\pi f_c (t - \tau_n(t))} \right\} \\ &= \Re\{r(t)e^{j2\pi f_c t}\}, \end{aligned}$$

where  $r(t)$  is the complex envelope of the received signal and can be represented as

$$r(t) = \sum_{n=1}^N \alpha_n(t) e^{-j2\pi f_c \tau_n(t)} x(t - \tau_n(t)). \quad (2.2.2)$$

Note that the complex envelopes,  $x(t)$  and  $r(t)$ , are respectively the equivalent representations of the transmitted and received narrowband signals at baseband. The channel can be characterized equivalently by its impulse response at baseband. Since the channel is time varying, the impulse response depends on the instant that the impulse is applied to the channel.

### 2.2.1 Channel Impulse Response

Let us first review the impulse response of a linear time-invariant (LTI) channel, as shown in Figure 2.5(a). Let  $h(t)$  denote the impulse response (i.e., the channel output when the channel input is an impulse applied at  $t = 0$ ,  $\delta(t)$ ). Here  $\delta(t)$  is the Dirac delta function and is defined by

$$\delta(t) = \begin{cases} 0, & t \neq 0 \\ \infty, & t = 0 \end{cases} \quad (2.2.3)$$

and

$$\int_{-\infty}^{\infty} \delta(t) dt = 1. \quad (2.2.4)$$

Because the channel is time invariant, if the input is delayed by  $t_1$ , the output is also delayed by  $t_1$  correspondingly. That is, the channel output in response to an input applied at time  $t_1$ ,  $\delta(t - t_1)$ ,

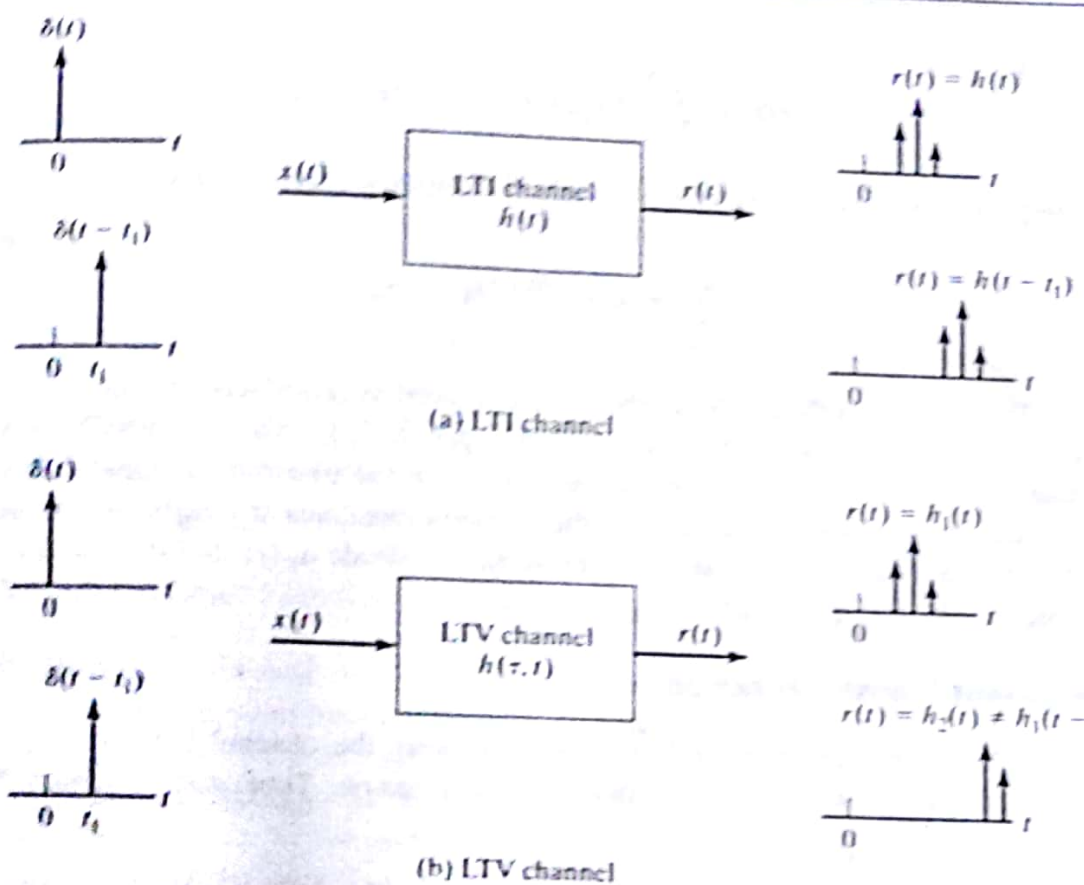


Figure 2.5 The linear channel model.

is  $h(t - t_1)$ . As a result, we can use the impulse response  $h(t)$  to completely characterize the channel. The time variable  $t$  in the impulse response actually represents the propagation delay of the channel. The channel output  $r(t)$  is given by

$$r(t) = h(t) * x(t) = \int_{-\infty}^{\infty} x(t - \tau)h(\tau) d\tau. \quad (2.2.5)$$

where  $*$  denotes the convolution operation.

Next consider an LTV channel, as shown in Figure 2.5(b), where  $h_1(t)$  and  $h_2(t)$  denote the channel responses to the inputs  $\delta(t)$  and  $\delta(t - t_1)$  respectively. As the channel propagation environment changes over the time duration  $[0, t_1]$ , the channel output  $h_2(t)$  is not simply  $h_1(t)$  delayed by  $t_1$  (i.e.,  $h_2(t) \neq h_1(t - t_1)$ ). As a result, in order to characterize an LTV channel, we should define a channel impulse response as a function of two time variables, one describing the instant when the impulse is applied to the channel (initial time), and the other describing the instant of observing the channel output (final time).

**Definition 2.1** The impulse response of an LTV channel,  $h(\tau, t)$ , is the channel output at  $t$  in response to an impulse applied to the channel at  $t - \tau$ .

In Definition 2.1, the variable  $\tau$  represents the propagation delay. From the definition and Eq. (2.2.5), the channel output can be represented in terms of the impulse response and the

channel input by

$$r(t) = \int_{-\infty}^{\infty} h(\tau, t)x(t - \tau)d\tau. \quad (2.2.6)$$

The channel impulse response for the channel with  $N$  distinct scatterers is then

$$h(\tau, t) = \sum_{n=1}^{N} \alpha_n(t)e^{-j\theta_n(t)}\delta(\tau - \tau_n(t)), \quad (2.2.7)$$

where  $\theta_n(t) = 2\pi f_c \tau_n(t)$  represents the carrier phase distortion introduced by the  $n$ th scatterer. Thus,  $\theta_n(t)$  changes by  $2\pi$  radians whenever  $\tau_n(t)$  changes by  $1/f_c$ , which is usually very small. This means that changes in  $\theta_n(t)$  have a far greater effect on the transmitted signal than changes in  $\alpha_n(t)$ , as a small change (such as motion) in the scatterer can cause a significant change in the phase  $\theta_n(t)$ , but may not cause significant changes in the amplitude  $\alpha_n(t)$ . Substituting Eq. (2.2.7) into Eq. (2.2.6), we obtain Eq. (2.2.2).

## 2.2.2 Time-Variant Transfer Function

With the multipath channel characterized as a linear system, the channel behavior can also be examined in the frequency domain via a Fourier transformation. Time and frequency have an inverse relationship.

**Definition 2.2** The time-variant transfer function of an LTV channel is the Fourier transform of the impulse response,  $h(\tau, t)$ , with respect to the delay variable  $\tau$ .

Let  $H(f, t)$  denote the channel transfer function, as shown in Figure 2.6. We have the Fourier transform pair

$$\begin{cases} H(f, t) = \mathcal{F}_{\tau}[h(\tau, t)] = \int_{-\infty}^{\infty} h(\tau, t)e^{-j2\pi f\tau}d\tau \\ h(\tau, t) = \mathcal{F}_f^{-1}[H(f, t)] = \int_{-\infty}^{\infty} H(f, t)e^{+j2\pi f\tau}df \end{cases}$$

where the time variable  $t$  can be viewed as a parameter. The received signal can be represented in terms of the transmitted signal and the transfer function as

$$r(t) = \int_{-\infty}^{\infty} R(f, t)e^{j2\pi ft}df, \quad (2.2.8)$$

where

$$R(f, t) = H(f, t)X(f)$$

and

$$X(f) = \mathcal{F}[x(t)].$$

At any instant, say  $t = t_0$ , the transfer function  $H(f, t_0)$  characterizes the channel in the frequency domain. As the channel changes with  $t$ , the frequency domain representation also

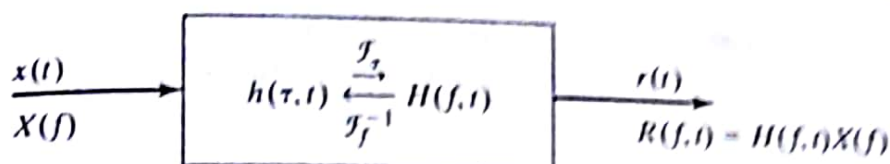


Figure 2.6 Frequency-time channel representation.

changes with  $t$ . Therefore, we have the channel time-varying transfer function. If the channel is time invariant, then the impulse response is a function of the delay variable  $\tau$  and is independent of the time variable  $t$ ; thus the transfer function varies only with the frequency variable  $f$  and is independent of  $t$ . This is consistent with the impulse response and transfer function of an LTI channel.

### 2.2.3 Doppler Spread Function and Delay-Doppler Spread Function

**Doppler Shifts** In general, the output signal of an LTI system does not have frequency components different from those of the input signal. That is, an LTI system does not introduce frequency shifts to its input signals. On the other hand, both nonlinear and time-varying systems introduce new frequency components other than those existing in the input signal. For a wireless propagation environment, due to the mobility of mobile users and/or the surrounding scatterers, the channel is linear but time variant. As a result, a wireless channel introduces frequency shifts to the transmitted signal, a phenomenon called the Doppler effect and the introduced frequency shifts called the Doppler shifts.

Consider a scenario shown in Figure 2.7, where the base station (BS) transmits a single-tone pilot signal at frequency  $f_c$ , and the mobile station (MS) is moving along the  $x$ -axis with a constant velocity  $V$ . Let  $\theta(t)$  denote the angle of the incoming pilot signal viewed from the

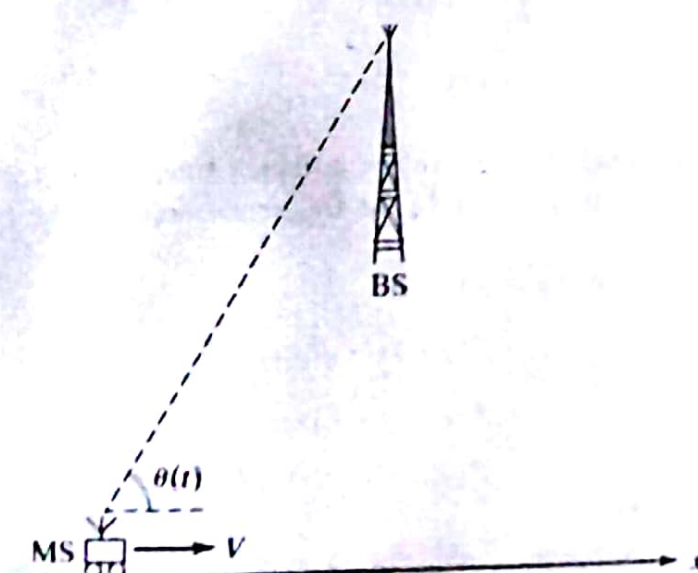


Figure 2.7 The Doppler effect.

mobile receiver at time  $t$ , with respect to the  $x$ -axis. The received signal at the mobile terminal at time  $t$  has a frequency of  $f_c + v(t)$ .  $v(t)$  is the Doppler shift and is given by

$$v(t) = \frac{Vf_c}{c} \cos \theta(t), \quad (2.2.9)$$

where  $c$  is the velocity of light. From Eq. (2.2.9), it is observed that the Doppler shift increases with the signal frequency  $f_c$  and user velocity  $V$ .

As a wireless channel can be characterized equivalently in both time and frequency domains, a channel being time varying in the time domain means a channel introducing Doppler shifts in the frequency domain. In fact, as a wireless channel usually introduces continuous Doppler shifts in a certain range including the zero Doppler shift, the effect of the channel on the transmitted signal in the frequency domain is more spectral broadening than a simple spectral shift. This phenomenon can be illustrated by the following simple example.

Consider the wireless channel with  $N$  distinct scatterers as described by Eq. (2.2.7). Assume that the delay spread is negligible as compared with the symbol interval of the transmitted signal. As a result, the propagation delay can be approximated by its mean value  $\bar{\tau}$ . For simplicity, we further assume that this mean delay does not change with time. The time-variant impulse response of the channel can be approximately described in the form

$$h(\tau, t) \approx Z(t)\delta(\tau - \bar{\tau}), \quad (2.2.10)$$

where  $Z(t) = \sum_{n=1}^N \alpha_n(t) \exp[-j2\pi f_c \tau_n(t)]$ . Given that the transmitted signal is  $x(t)$ , the received signal in the absence of background noise is

$$\begin{aligned} r(t) &= \int_{-\infty}^{\infty} h(\tau, t)x(t - \tau) d\tau \\ &= \int_{-\infty}^{\infty} [Z(t)\delta(\tau - \bar{\tau})]x(t - \tau) d\tau \\ &= Z(t)x(t - \bar{\tau}). \end{aligned}$$

The overall effect of the channel is to provide a complex time-varying gain,  $Z(t)$ , and a transmission delay,  $\bar{\tau}$ , to the transmitted signal. In the frequency domain, the received signal is

$$\begin{aligned} R(f) &= \mathcal{F}[r(t)] \\ &= \mathcal{F}[Z(t)x(t - \bar{\tau})] \\ &= \mathcal{F}[Z(t)] * \mathcal{F}[x(t - \bar{\tau})] \\ &= \mathcal{F}[Z(t)] * [X(f)e^{-j2\pi f \bar{\tau}}], \end{aligned}$$

where  $X(f) = \mathcal{F}[x(t)]$ . Given that the channel gain  $Z(t)$  changes with time, its Fourier transform  $\mathcal{F}[Z(t)]$  has a finite but nonzero pulse width in the frequency domain. As a result, the pulse width of  $R(f)$  is larger than the pulse width of  $X(f)$  due to the convolution operation. This means

that the channel indeed broadens the transmitted signal spectrum by introducing new frequency components, a phenomenon referred to as frequency dispersion.

**Doppler Spread Function  $H(f, v)$ .** An LTV wireless channel can be characterized by the Doppler spread function  $H(f, v)$  which is defined by the relation between the channel input signal and output signal in the frequency domain. Let  $X(f)$  and  $R(f)$  denote the Fourier transforms of the transmitted signal  $x(t)$  and received signal  $r(t)$ , respectively. Then  $H(f, v)$  is defined by the following equation

$$R(f) = \int_{-\infty}^{\infty} X(f - v) H(f - v, v) dv, \quad (2.2.11)$$

where  $v$  is a variable describing the Doppler shift introduced by the channel. From Eq. (2.2.11),  $H(f, v)$  is the channel gain associated with Doppler shift  $v$  to the input signal component at frequency  $f$ . Since both the time-variant transfer function  $H(f, t)$  and the Doppler spread function  $H(f, v)$  can be used to describe the same channel, there exists a relation between the two channel functions. It can be shown that

$$\begin{cases} H(f, v) = \mathcal{F}_t[H(f, t)] = \int_{-\infty}^{\infty} H(f, t) e^{-j2\pi vt} dt \\ H(f, t) = \mathcal{F}_v^{-1}[H(f, v)] = \int_{-\infty}^{\infty} H(f, v) e^{+j2\pi vt} dv \end{cases}$$

where the frequency variable  $f$  can be viewed as a parameter. The preceding Fourier transform relation verifies that being time-variant in the time domain can be equivalently described by having Doppler shifts in the frequency domain.

**Delay-Doppler Spread Function.** A wireless channel can be characterized by the delay-Doppler spread function  $H(\tau, v)$  defined as the Fourier transform of the channel impulse response  $h(\tau, t)$  with respect to  $t$ , as follows:

$$H(\tau, v) = \mathcal{F}_t[h(\tau, t)] = \int_{-\infty}^{\infty} h(\tau, t) e^{-j2\pi vt} dt. \quad (2.2.12)$$

Given the channel input signal  $x(t)$ , it can be shown that the channel output signal is

$$r(t) = \int_{-\infty}^{\infty} \int_{-\infty}^{\infty} x(t - \tau) H(\tau, v) e^{j2\pi vt} dv d\tau. \quad (2.2.13)$$

As both the transmitted signal and received signal can be represented either in the time domain or in the frequency domain, we have four channel functions,  $h(\tau, t)$ ,  $H(f, t)$ ,  $H(\tau, v)$ , and  $H(f, v)$  to characterize the relation between the transmitted signal and the received signal. These four functions are equivalent in describing the LTV channel. Preference in selecting any one of the functions depends on whether the transmitted and received signals are represented

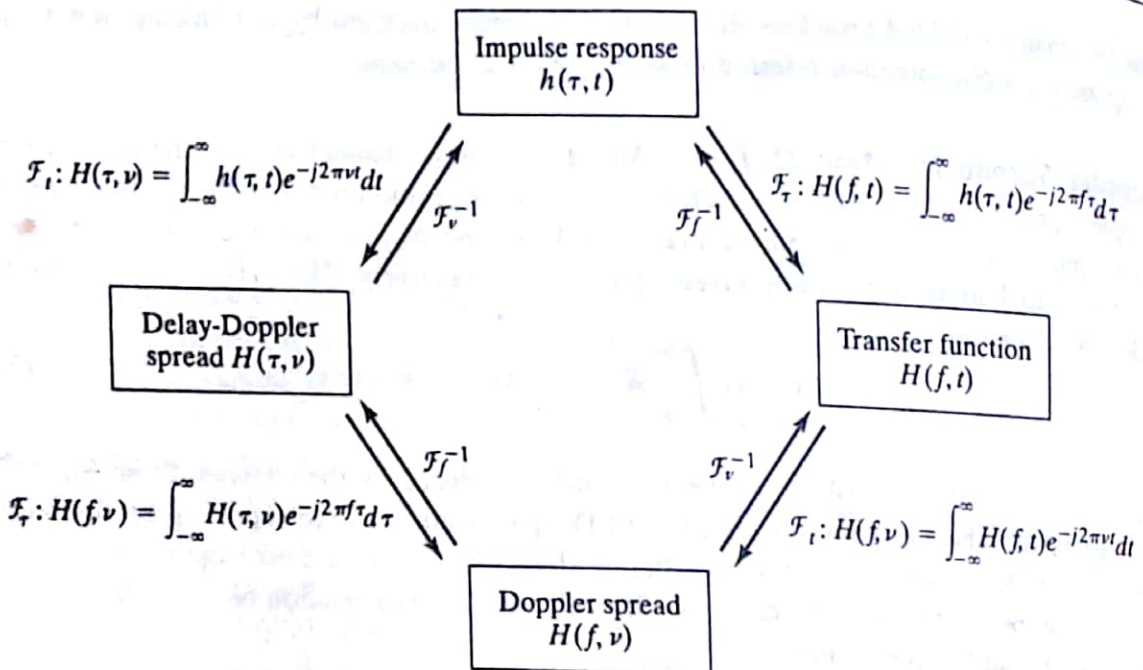


Figure 2.8 Relationships among the channel functions.

in the time or frequency domain. Figure 2.8 summarizes the relationships among the channel functions.

## 2.2.4 Example on the Channel Functions

### Example 2.1 LTV Channel Model

Consider an LTV channel with impulse response given by

$$h(\tau, t) = 4 \exp(-\tau/T) \cos(\Omega t), \quad \tau \geq 0, \quad (2.2.14)$$

where  $T = 0.1$  ms and  $\Omega = 10\pi$ .

- Find the channel time-variant transfer function  $H(f, t)$  and the Doppler spread function  $H(f, \nu)$ .
- Given that the transmitted signal is

$$x_1(t) = \begin{cases} 1, & |t| \leq T_0 \\ 0, & |t| > T_0 \end{cases}, \quad (2.2.15)$$

- where  $T_0 = 0.025$  ms, find the received signal in the absence of background noise.
- Repeat part (b) if the transmitted signal is

$$x_2(t) = x_1(t - T_1), \quad (2.2.16)$$

- where  $T_1 = 0.05$  ms.
- What do you observe from the results of parts (b) and (c)?

**Solution**

- a. The time-variant transfer function is

$$\begin{aligned}
 H(f, t) &= \mathcal{F}_\tau[h(\tau, t)] \\
 &= \mathcal{F}_\tau[4 \exp(-\tau/T) \cos(\Omega\tau)], \quad \tau \geq 0 \\
 &= 4 \cos(\Omega t) \mathcal{F}_\tau[\exp(-\tau/T)], \quad \tau \geq 0 \\
 &= \frac{4T \cos(\Omega t)}{1 + j2\pi f T}.
 \end{aligned}$$

The Doppler spread function is

$$\begin{aligned}
 H(f, v) &= \mathcal{F}_t[H(f, t)] \\
 &= \mathcal{F}_t\left[\frac{4T \cos(\Omega t)}{1 + j2\pi f T}\right] \\
 &= \frac{4T}{1 + j2\pi f T} \mathcal{F}_t[\cos(\Omega t)] \\
 &= \frac{2T}{1 + j2\pi f T} [\delta(2\pi v + \Omega) + \delta(2\pi v - \Omega)].
 \end{aligned}$$

- b. The received signal is calculated as follows:

$$\begin{aligned}
 r_1(t) &= \int_{-\infty}^{\infty} h(\tau, t) x_1(t - \tau) d\tau \\
 &= \int_0^{\infty} 4 \exp(-\tau/T) \cos(\Omega\tau) x_1(t - \tau) d\tau \\
 &= \begin{cases} 0, & t \leq -T_0 \\ 4T \cos(\Omega t) \left[ 1 - \exp\left(-\frac{t+T_0}{T}\right) \right], & -T_0 < t < T_0 \\ 4T \cos(\Omega t) \left[ \exp\left(-\frac{t-T_0}{T}\right) - \exp\left(-\frac{t+T_0}{T}\right) \right], & t \geq T_0 \end{cases}
 \end{aligned}$$

The transmitted and received signals are plotted in Figure 2.9(a).

- c. Similar to part (b), the received signal is calculated as follows:

$$\begin{aligned}
 r_2(t) &= \int_{-\infty}^{\infty} h(\tau, t) x_2(t - \tau) d\tau \\
 &= \int_0^{\infty} 4 \exp(-\tau/T) \cos(\Omega\tau) x_2(t - T_1 - \tau) d\tau
 \end{aligned}$$

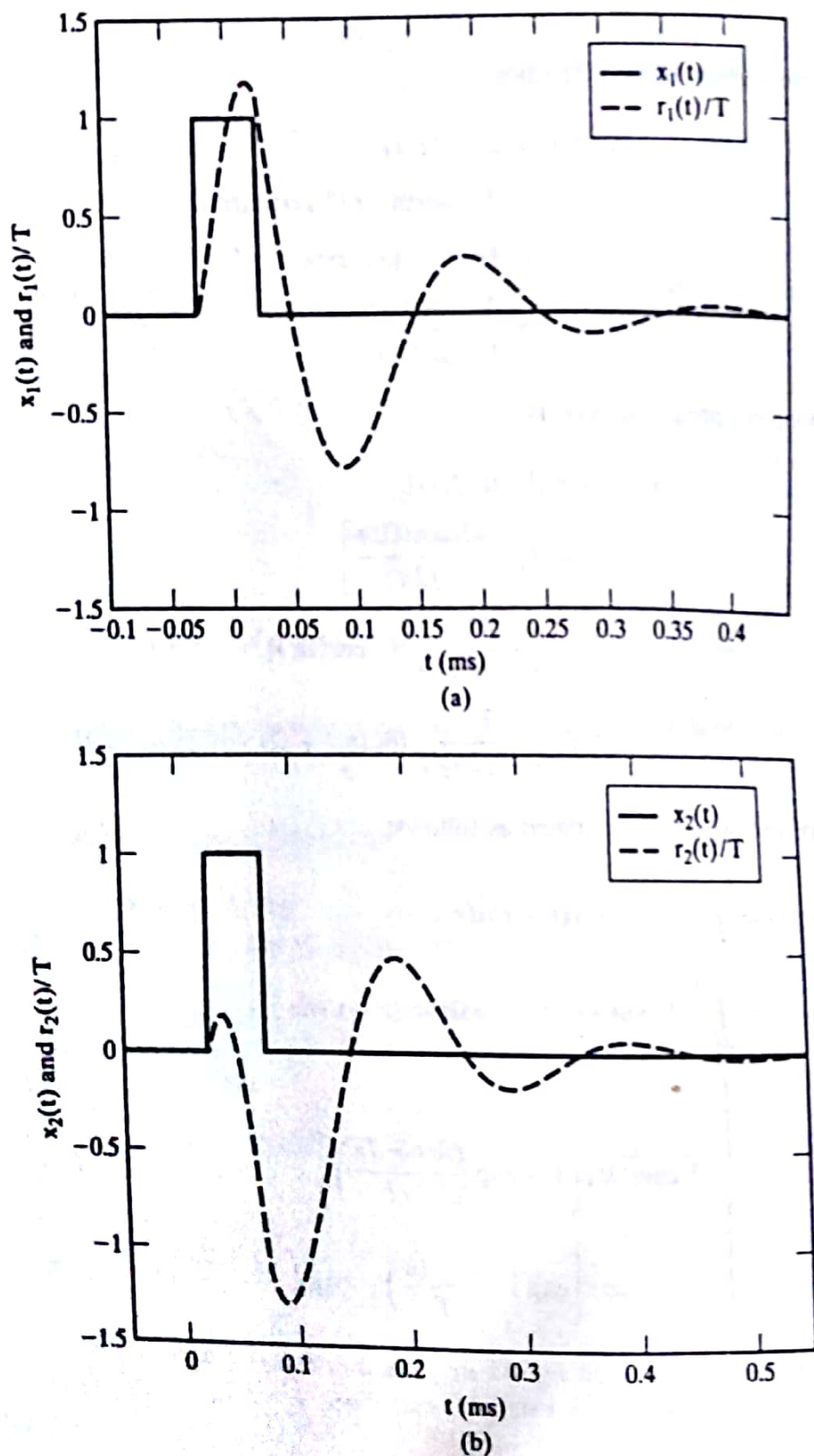


**Figure 2.9** The transmitted signals  $x_i(t)$  and normalized received signals  $r_i(t)/T$  ( $i = 1$  and  $2$ ) in Example 2.1.

$$= \begin{cases} 0, & t \leq T_1 - T_0 \\ 4T \cos(\Omega t) \left[ 1 - \exp\left(-\frac{t - T_1 + T_0}{T}\right) \right], & T_1 - T_0 < t < T_1 + T_0 \\ 4T \cos(\Omega t) \left[ \exp\left(-\frac{t - T_1 - T_0}{T}\right) - \exp\left(-\frac{t - T_1 + T_0}{T}\right) \right], & t \geq T_1 + T_0 \end{cases}$$

The transmitted and received signals are plotted in Figure 2.9(b).

- d. From Figure 2.9, it is observed that: (1) the received signals have a larger pulse width than the corresponding transmitted signals because the channel is time dispersive; and (2) even though the transmitted signal  $x_2(t)$  is  $x_1(t)$  delayed by  $T_1$ , the received signal  $r_2(t)$  is not  $r_1(t)$  delayed by  $T_1$  because the channel is time varying.

## 2.3 CHANNEL CORRELATION FUNCTIONS

When the channel changes with time randomly, the channel impulse response  $h(\tau, t)$ , time-variant transfer function  $H(f, t)$ , Doppler spread function  $H(f, v)$ , and delay-Doppler spread function  $H(\tau, v)$  are random processes and are difficult to characterize. Under the assumption that the random processes have zero mean, we are interested in the correlation functions of the random processes. For simplicity of analysis, we assume that

- a. the channel impulse response  $h(\tau, t)$  is a wide-sense stationary (WSS) process;
- b. the channel impulse responses at  $\tau_1$  and  $\tau_2$ ,  $h(\tau_1, t)$  and  $h(\tau_2, t)$ , are uncorrelated if  $\tau_1 \neq \tau_2$  for any  $t$ .

A channel under assumptions (a) and (b) is said to be a wide-sense stationary uncorrelated scattering (WSSUS) channel.

### 2.3.1 Delay Power Spectral Density

Under assumption (a), the autocorrelation function of  $h(\tau, t)$ , defined as

$$\frac{1}{2} E[h^*(\tau_1, t)h(\tau_2, t + \Delta t)],$$

is a function of  $\tau_1$ ,  $\tau_2$ , and  $\Delta t$ , and does not depend on  $t$ . The superscript (\*) denotes complex conjugation. The correlation function can be represented as

$$\phi_h(\tau_1, \tau_2, \Delta t) \stackrel{\Delta}{=} \frac{1}{2} E[h^*(\tau_1, t)h(\tau_2, t + \Delta t)]. \quad (2.3.1)$$

Furthermore, under assumption (b), the autocorrelation function can be represented in the form [12]

$$\phi_h(\tau_1, \tau_2, \Delta t) = \phi_h(\tau_1, \Delta t)\delta(\tau_1 - \tau_2), \quad (2.3.2)$$

or equivalently,

$$\phi_h(\tau, \tau + \Delta \tau, \Delta t) = \phi_h(\tau, \Delta t)\delta(\Delta \tau), \quad (2.3.3)$$

where

$$\phi_h(\tau, \Delta t) = \int \phi_h(\tau, \tau + \Delta \tau, \Delta t) d\Delta \tau.$$

At  $\Delta t = 0$ , we define

$$\phi_h(\tau) \stackrel{\Delta}{=} \phi_h(\tau, 0). \quad (2.3.4)$$

From Eqs. (2.3.1)–(2.3.4), we have

$$\begin{aligned} \phi_h(\tau) &= \mathcal{F}_{\Delta \tau}[\phi_h(\tau, \tau + \Delta \tau, \Delta t)]|_{\Delta t=0} \\ &= \mathcal{F}_{\Delta \tau} \left\{ \frac{1}{2} E[h^*(\tau, t)h(\tau + \Delta \tau, t)] \right\}. \end{aligned} \quad (2.3.5)$$

From Eq. (2.3.5), we observe that  $\phi_h(\tau)$  is the Fourier transform of the correlation function. According to the Wiener-Khintchine relations<sup>1</sup>, the function  $\phi_h(\tau)$  represents power spectral density (psd). It measures the average psd at the channel output as a function of the propagation delay,  $\tau$ , and is therefore called the delay psd of the channel, also known as the multipath intensity profile. Figure 2.10 illustrates an example of the psd, where the minimum delay is assumed to be zero. The nominal width of the delay psd pulse is called the multipath delay spread, denoted by  $T_m$ .

From the delay psd, we can calculate statistics describing the time dispersive characteristics of the channel. The  $n$ th moment of the delay, denoted by  $\bar{\tau}^n$ , is given by

$$\bar{\tau}^n = \frac{\int \tau^n \phi_h(\tau) d\tau}{\int \phi_h(\tau) d\tau}. \quad (2.3.6)$$

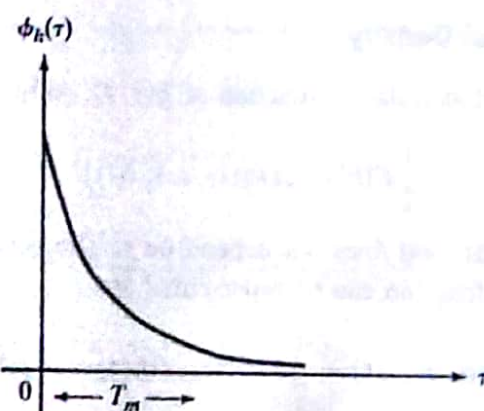


Figure 2.10 Delay power spectral density.

<sup>1</sup>For a WSS random process, its power spectral density in the frequency domain is the Fourier transform of its autocorrelation function in the time domain. The relations between the autocorrelation function and the power spectral density are called the Wiener-Khintchine relations.

The mean propagation delay, or first moment, denoted by  $\bar{\tau}$ , is

$$\bar{\tau} = \frac{\int \tau \phi_h(\tau) d\tau}{\int \phi_h(\tau) d\tau}, \quad (2.3.7)$$

and the rms (root-mean-square) delay spread, denoted by  $\sigma_\tau$ , is

$$\sigma_\tau = \left[ \frac{\int (\tau - \bar{\tau})^2 \phi_h(\tau) d\tau}{\int \phi_h(\tau) d\tau} \right]^{1/2} \quad (2.3.8)$$

In calculating a value for the multipath delay spread, it is usually assumed that

$$T_m \approx \sigma_\tau.$$

In the preceding calculations, the contribution of each delay  $\tau$  to the statistics is weighted by the psd level associated with the delay, and is normalized by the total power  $\int \phi_h(\tau) d\tau$ .

### 2.3.2 Frequency and Time Correlation Functions

From the relationship between  $h(\tau, t)$  and  $H(f, t)$ , we have the following:

- a. If  $h(\tau, t)$  is WSS, then  $H(f, t)$  is also WSS with respect to  $t$ . As a result, we can define the autocorrelation function of the time-variant transfer function  $H(f, t)$  as

$$\phi_H(f_1, f_2, \Delta t) \triangleq \frac{1}{2} E[H^*(f_1, t) H(f_2, t + \Delta t)]. \quad (2.3.9)$$

- b. The correlation function  $\phi_H(f_1, f_2, \Delta t)$  can be represented in terms of the correlation function  $\phi_h(\tau, \Delta t)$ .

$$\begin{aligned} \phi_H(f_1, f_2, \Delta t) &= \int_{-\infty}^{\infty} \phi_h(\tau, \Delta t) e^{-j2\pi(f_2 - f_1)\tau} d\tau \\ &= \int_{-\infty}^{\infty} \phi_h(\tau, \Delta t) e^{-j2\pi(\Delta f)\tau} d\tau \\ &\triangleq \phi_H(\Delta f, \Delta t), \end{aligned}$$

where  $\Delta f = f_2 - f_1$ .

The function  $\phi_H(\Delta f, \Delta t)$  is a time-frequency correlation function. Letting  $\Delta t = 0$ , we can write the frequency domain representation as a Fourier transform of the delay psd, i.e.,

$$\begin{aligned} \phi_H(\Delta f) &\triangleq \frac{1}{2} E[H^*(f, t) H(f + \Delta f, t)] \\ &= \int_{-\infty}^{\infty} \phi_h(\tau) e^{-j2\pi(\Delta f)\tau} d\tau. \end{aligned} \quad (2.3.10)$$

$\phi_H(\Delta f)$  is called the frequency correlation function of the wireless channel. The delay PSD,  $\phi_h(\tau)$ , portrays the time domain behavior of the fading channel, whereas the frequency correlation function,  $\phi_H(\Delta f)$ , portrays the frequency domain behavior. The nominal width of  $\phi_H(\Delta f)$ , denoted by  $(\Delta f)_c$ , is called the channel coherence bandwidth, as shown in Figure 2.11. Since time and frequency have an inverse relationship, we have

$$(\Delta f)_c \approx \frac{1}{T_m} \quad (2.3.11)$$

(i.e., a large multipath delay spread also means a small channel coherence bandwidth).

Over the channel coherence bandwidth, all signal frequency components experience the correlated perturbation. When a signal propagates through the channel, the frequency components of the signal separated by a frequency width greater than the channel coherence bandwidth are distorted by the channel in an uncorrelated manner. The degree of fading experienced by the transmitted signal depends on the relationship between the channel coherence bandwidth and the transmitted signal bandwidth. Let  $W_s$  denote the bandwidth of the transmitted signal. The fading channel can be grossly categorized as follows:

- If  $(\Delta f)_c < W_s$ , the channel is said to exhibit frequency selective fading which introduces severe ISI to the received signal;
- If  $(\Delta f)_c \gg W_s$ , the channel is said to exhibit frequency nonselective fading or flat fading which introduces negligible ISI.

In the time-frequency correlation function  $\phi_H(\Delta f, \Delta t)$ , letting  $\Delta f = 0$ , we have

$$\phi_H(\Delta t) \triangleq \phi_H(0, \Delta t) = \frac{1}{2} E[H^*(f, t)H(f, t + \Delta t)]. \quad (2.3.12)$$

$\phi_H(\Delta t)$  is called the time correlation function of the channel. It characterizes, on average, how fast the channel transfer function changes with time at each frequency. The nominal width of  $\phi_H(\Delta t)$  is called the coherence time of the fading channel, denoted by  $(\Delta t)_c$ , as shown in Figure 2.12.

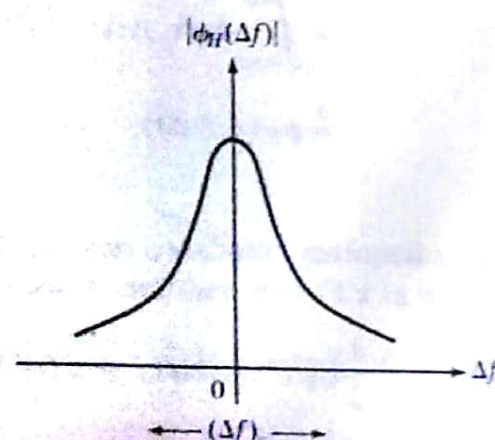
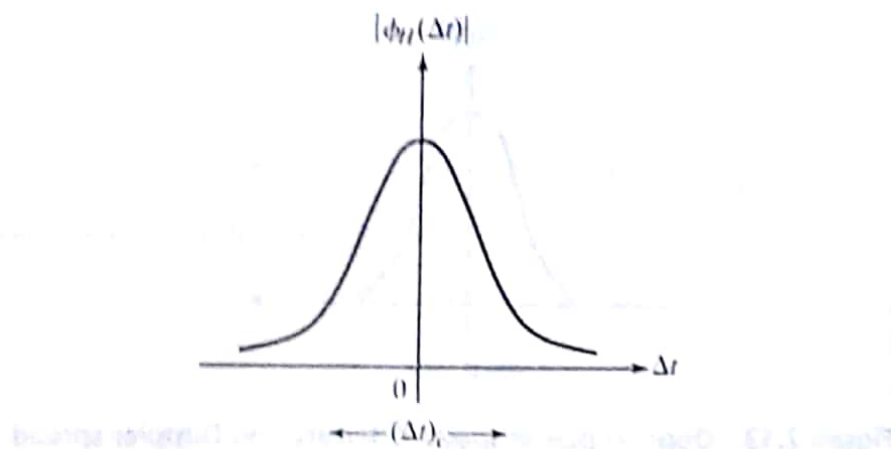


Figure 2.11 Frequency-correlation function and channel coherence bandwidth.



**Figure 2.12** Time-correlation function and channel coherence time.

The channel fading at time  $t$  will be very different from that at time  $t - (\Delta t)_c$  or earlier. If the channel coherence time is much larger than the symbol interval of the transmitted signal, the channel exhibits slow fading to the signal because the channel changing rate is much smaller than the transmission symbol rate. The time correlation function is independent of the frequency variable  $f$  due to the assumption that the channel has uncorrelated scattering. In other words, a channel exhibiting uncorrelated scattering in the time domain can be described equivalently as the condition that the channel transfer function is WSS in the frequency domain (with respect to  $f$ ).

### 2.3.3 Doppler Power Spectral Density

The correlation function of the Doppler spread function  $H(f, v)$  is defined as

$$\frac{1}{2} E[H^*(f_1, v_1)H(f_2, v_2)].$$

For a WSSUS channel, the correlation function can be represented in the form [12]

$$\Phi_H(\Delta f, v_1)\delta(v_1 - v_2),$$

where  $\Delta f = f_2 - f_1$  and  $\Phi_H(\Delta f, v)$  can be obtained by Fourier transformation of the frequency-time correlation function  $\phi_H(\Delta f, \Delta t)$  with respect to  $\Delta t$ . Therefore,

$$\Phi_H(\Delta f, v) = \int_{-\infty}^{\infty} \phi_H(\Delta f, \Delta t) e^{-j2\pi v \Delta t} d\Delta t. \quad (2.3.13)$$

At  $\Delta f = 0$ , we have

$$\Phi_H(v) \triangleq \Phi_H(0, v) = \int_{-\infty}^{\infty} \phi_H(\Delta t) e^{-j2\pi v \Delta t} d\Delta t. \quad (2.3.14)$$

Equation (2.3.14) shows that the correlation function  $\Phi_H(v)$  is the Fourier transform of the channel correlation function  $\phi_H(\Delta t)$ . Based on the Wiener-Khintchine relations,  $\Phi_H(v)$  is a psd in terms

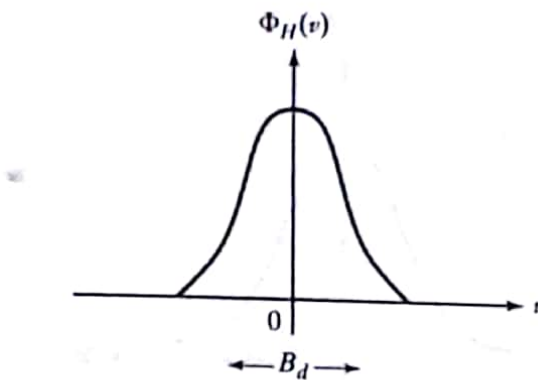


**Figure 2.13** Doppler power spectral density and Doppler spread.

of the Doppler shift  $v$ . As a result, the function  $\Phi_H(v)$  is called the Doppler psd. The nominal width of the Doppler psd, denoted by  $B_d$ , is called the Doppler spread, as shown in Figure 2.13. From the relation that  $\phi_H(\Delta t)$  and  $\Phi_H(v)$  are a Fourier transform pair, we see that the coherence time is inversely proportional to the Doppler spread,

$$(\Delta t)_c \approx \frac{1}{B_d}. \quad (2.3.15)$$

With the Doppler psd, the  $n$ th moment of Doppler shift, denoted by  $\bar{v}^n$ , can be calculated by

$$\bar{v}^n = \frac{\int v^n \Phi_H(v) dv}{\int \Phi_H(v) dv}. \quad (2.3.16)$$

The mean Doppler shift, or the first moment, denoted by  $\bar{v}$ , is

$$\bar{v} = \frac{\int v \Phi_H(v) dv}{\int \Phi_H(v) dv}, \quad (2.3.17)$$

and the rms Doppler spread, denoted by  $\sigma_v$ , is

$$\sigma_v = \left[ \frac{\int (v - \bar{v})^2 \Phi_H(v) dv}{\int \Phi_H(v) dv} \right]^{1/2} \quad (2.3.18)$$

As an approximation, it is usually assumed that

$$B_d \approx \sigma_v.$$

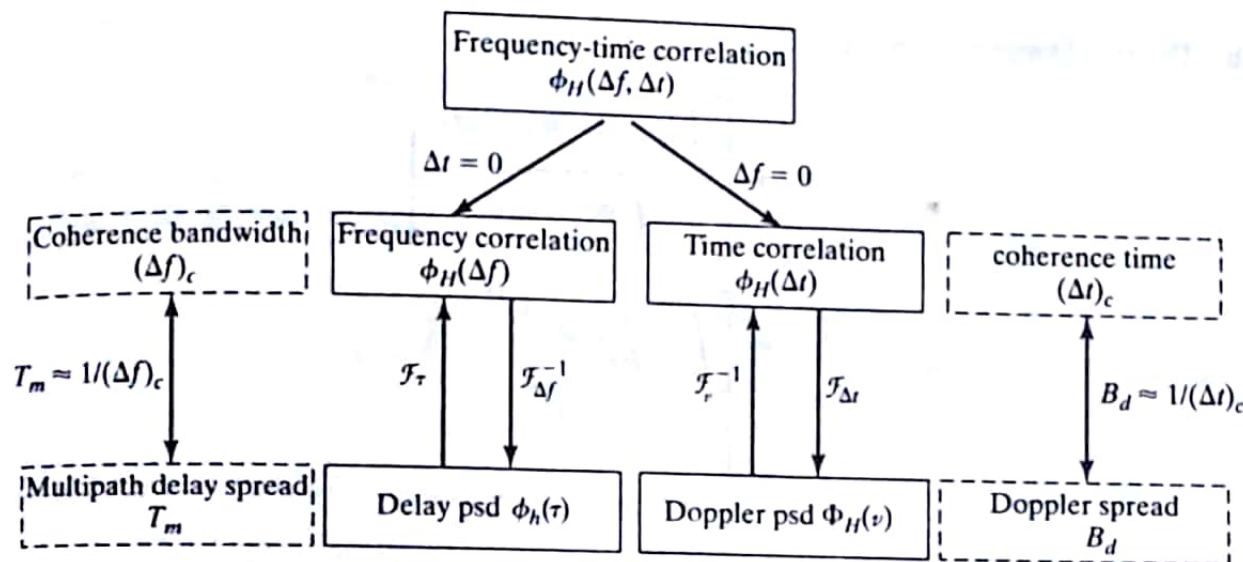


**Figure 2.14** Relationships between the channel correlation functions and between the channel parameters.

Figure 2.14 summarizes the relationships between the correlation functions and power spectral densities and between the channel parameters.

### 2.3.4 Examples on the Channel Correlation Functions

#### Example 2.2 Calculation of the Channel Parameters

Consider a fading channel which exhibits a Doppler frequency shift uniformly distributed between -10 Hz and 10 Hz. Determine

- the mean Doppler shift,
- the rms Doppler spread, and
- the coherence time.

**Solution** The Doppler psd normalized with respect to the total power is

$$\Phi_H(v) = \begin{cases} \frac{1}{20}, & -10 < v < 10 \\ 0, & \text{elsewhere.} \end{cases}$$

- The mean Doppler shift is

$$\bar{v} = \frac{\int_{-10}^{10} \frac{1}{20} v dv}{\int_{-10}^{10} \frac{1}{20} dv} = \frac{\frac{v^2}{40} \Big|_{-10}^{10}}{1} = 0.$$

b. The rms Doppler spread is

$$\begin{aligned}\sigma_v &= \left[ \frac{\int (v - \bar{v})^2 \Phi_H(v) dv}{\int \Phi_H(v) dv} \right]^{1/2} \\ &= \left[ \int_{-10}^{10} \frac{1}{20} v^2 dv \right]^{1/2} \\ &= \left[ \frac{v^3}{60} \Big|_{-10}^{10} \right]^{1/2} \\ &= 5.77 \text{ Hz.}\end{aligned}$$

c. The channel coherence time is

$$(\Delta t)_c \approx \frac{1}{B_d} \approx \frac{1}{\sigma_v} = \frac{1}{5.77} = 0.1733 \text{ s.}$$

### Example 2.3 Delay PSD and Frequency-Correlation Function

Consider a WSSUS channel whose time-variant impulse response is given by

$$h(\tau, t) = \exp(-\tau/T) n(\tau) \cos(\Omega t + \Theta), \quad \tau \geq 0,$$

where  $T$  and  $\Omega$  are constants,  $\Theta$  is a random variable uniformly distributed in  $[-\pi, +\pi]$ , and  $n(\tau)$  is a real-valued random process independent of  $\Theta$ , with  $E[n(\tau)] = \mu_n$  and  $E[n(\tau_1)n(\tau_2)] = \delta(\tau_1 - \tau_2)$ .

- a. Calculate the delay psd and the multipath delay spread.
- b. Calculate the frequency correlation function and the channel coherence bandwidth.
- c. Determine whether the channel exhibits frequency-selective fading for GSM systems with  $T = 0.1$  ms.

#### Solution

- a. From Eq. (2.3.5), we have

$$\begin{aligned}\phi_h(\tau) &= \mathcal{F}_{\Delta\tau} \left\{ \frac{1}{2} E[h^*(\tau, t) h(\tau + \Delta\tau, t)] \right\} \\ &= \mathcal{F}_{\Delta\tau} \left\{ \frac{1}{2} E[n(\tau) n(\tau + \Delta\tau)] E[e^{-(2\tau + \Delta\tau)/T} \cos^2(\Omega t + \Theta)] \right\}, \quad \tau \geq 0 \\ &= \mathcal{F}_{\Delta\tau} \left\{ \frac{1}{4} e^{-(2\tau + \Delta\tau)/T} \delta(\Delta\tau) E[1 + \cos(2\Omega t + 2\Theta)] \right\}, \quad \tau \geq 0 \\ &= \frac{1}{4} e^{-2\tau/T}, \quad \tau \geq 0,\end{aligned}$$

where

$$E[\cos(2\Omega t + 2\theta)] = \int_{-\pi}^{+\pi} \cos(2\Omega t + 2\theta) \frac{1}{2\pi} d\theta = 0.$$

For  $\tau < 0$ ,  $\phi_h(\tau) = 0$ .

The mean propagation delay is

$$\bar{\tau} = \frac{\int_0^\infty \tau \phi_h(\tau) d\tau}{\int_0^\infty \phi_h(\tau) d\tau} = \frac{\int_0^\infty \tau \frac{1}{4} e^{-2\tau/T} d\tau}{\int_0^\infty \frac{1}{4} e^{-2\tau/T} d\tau} = \frac{T}{2}$$

and the multipath delay spread is

$$T_m \approx \sigma_\tau = \left[ \frac{\int (\tau - \bar{\tau})^2 \phi_h(\tau) d\tau}{\int \phi_h(\tau) d\tau} \right]^{1/2} = \left[ \frac{\int \tau^2 \phi_h(\tau) d\tau}{\int \phi_h(\tau) d\tau} - \bar{\tau}^2 \right]^{1/2} = \frac{T}{2}.$$

b. The frequency correlation function is

$$\begin{aligned} \phi_H(\Delta f) &= \mathcal{F}[\phi_h(\tau)] \\ &= \int_0^\infty \frac{1}{4} e^{-2\tau/T} e^{-j2\pi(\Delta f)\tau} d\tau \\ &= \frac{T}{8 + j8\pi T(\Delta f)}. \end{aligned}$$

The coherence bandwidth is

$$(\Delta f)_c \approx 1/T_m = \frac{2}{T}.$$

- c. With  $T = 0.1$  ms, we have  $(\Delta f)_c = 20$  kHz. The GSM channels have a bandwidth of 200 kHz. Since  $(\Delta f)_c \ll 200$  kHz, the channel fading is frequency selective.

#### Example 2.4 Doppler PSD

For the channel specified in Example 2.3 with  $\Omega = 10\pi$ , find

- the Doppler psd,
- the mean Doppler shift and the rms Doppler spread,
- the channel coherence time, and
- whether the channel exhibits slow fading for GSM systems.

Solution

- The Doppler psd can be calculated by taking the Fourier transform of the time correlation function  $\phi_H(\Delta t)$ . In this way, we need to calculate the correlation function  $\phi_h(\tau, \Delta t)$  first.

For the WSS channel, from Eqs. (2.3.1)–(2.3.5), we have for  $\tau \geq 0$

$$\begin{aligned}\phi_h(\tau, \Delta t) &= \mathcal{F}_{\Delta t} \left\{ \frac{1}{2} E[h^*(\tau, t) h(\tau + \Delta t, t + \Delta t)] \right\} \\ &= \mathcal{F}_{\Delta t} \left\{ \frac{1}{2} E[e^{-\tau/T} n(\tau) \cos(\Omega t + \Theta) \right. \\ &\quad \cdot e^{-(\tau+\Delta t)/T} n(\tau + \Delta t) \cos(\Omega t + \Omega \Delta t + \Theta)] \Big\} \\ &= \mathcal{F}_{\Delta t} \left\{ \frac{1}{4} e^{-(2\tau+\Delta t)/T} E[n(\tau) n(\tau + \Delta t)] E[\cos(\Omega \Delta t) \right. \\ &\quad \left. + \cos(2\Omega t + \Omega \Delta t + 2\Theta)] \right\} \\ &= \mathcal{F}_{\Delta t} \left\{ \frac{1}{4} e^{-(2\tau+\Delta t)/T} \delta(\Delta t) \cos(\Omega \Delta t) \right\} \\ &= \frac{1}{4} e^{-2\tau/T} \cos(\Omega \Delta t), \quad \tau \geq 0.\end{aligned}$$

The time correlation function is then

$$\begin{aligned}\phi_H(\Delta t) &= \phi_H(\Delta f, \Delta t)|_{\Delta f=0} \\ &= \int_{-\infty}^{\infty} \phi_h(\tau, \Delta t) d\tau \\ &= \frac{1}{4} \cos(\Omega \Delta t) \int_0^{\infty} e^{-2\tau/T} d\tau \\ &= \frac{T}{8} \cos(\Omega \Delta t).\end{aligned}$$

The Doppler psd is

$$\begin{aligned}\Phi_H(v) &= \mathcal{F}[\phi_H(\Delta t)] \\ &= \mathcal{F} \left[ \frac{T}{8} \cos(\Omega \Delta t) \right] \\ &= \frac{T}{16} [\delta(2\pi v - \Omega) + \delta(2\pi v + \Omega)].\end{aligned}$$

That is, the channel introduces two Doppler shifts,  $\pm \Omega/2\pi = \pm 5$  Hz, with equal psd.

- b. The mean Doppler shift is zero as the two Doppler shifts are negative of each other and have the same psd. This can also be verified by using Eq. (2.3.17) and the psd computed

in (a). From Eq. (2.3.18), the rms Doppler spread is

$$\begin{aligned}\sigma_v &= \left\{ \frac{\int_{-\infty}^{\infty} v^2 \cdot \frac{T}{16} [\delta(2\pi v - \Omega) + \delta(2\pi v + \Omega)] dv}{\int_{-\infty}^{\infty} \frac{T}{16} [\delta(2\pi v - \Omega) + \delta(2\pi v + \Omega)] dv} \right\}^{1/2} \\ &= \left\{ \frac{\frac{T}{16} \left[ \left(\frac{\Omega}{2\pi}\right)^2 + \left(-\frac{\Omega}{2\pi}\right)^2 \right]}{\frac{T}{16}[1+1]} \right\}^{1/2} \\ &= \frac{\Omega}{2\pi},\end{aligned}$$

which is 5 Hz.

c. The coherence time is

$$(\Delta t)_c \approx \frac{1}{\sigma_v} = 0.2 \text{ s.}$$

d. In GSM systems, the data rate  $R_s = 270.833 \text{ kbps}$ , which corresponds to a symbol interval

$$T_s = \frac{1}{R_s} \approx 3.7 \times 10^{-6} \text{ s.}$$

Since  $T_s \ll (\Delta t)_c$ , the channel exhibits slow fading.

## 2.4 LARGE-SCALE PATH LOSS AND SHADOWING

The channel functions in a wireless environment are random processes and are very difficult to characterize. As a result, in Section 2.3, we focus only on the channel correlation functions. In the following, we will study the channel from a different point of view: At any instant (or distance), the channel impulse response is a random variable. We are interested in describing the channel at any time  $t$  (or distance  $d$ ) using a probability density function (pdf) under some assumptions.

Consider a flat fading channel where the multipath delay spread is very small compared with the symbol interval of the transmitted signal. The channel impulse response can be approximated by

$$h(\tau, t) \approx h(\bar{\tau}, t) \stackrel{\Delta}{=} g(t)\delta(\tau - \bar{\tau}), \quad (2.4.1)$$

where  $\bar{\tau}$  is the mean delay and is assumed to be time invariant. Given that the transmitted signal is  $x(t)$ , from Eq. (2.2.6), the received signal is

$$r(t) = \int_{-\infty}^{\infty} h(\tau, t)x(t - \tau) d\tau \approx g(t)x(t - \bar{\tau}). \quad (2.4.2)$$

In addition to the delay  $\bar{\tau}$ , the channel provides a time-varying gain  $g(t)$  to the transmitted signal. In general, the channel gain can be decomposed into a small-scale (or short-term) fading component,  $Z(t)$ , and a path loss with large-scale (or long-term) shadowing component (representing the local mean), as depicted in Figure 2.15. The short-term fading is due to multipath propagation and is independent of the distance between the transmitter and receiver. It can be characterized by a Rayleigh, Rician or Nakagami distribution [103]. The path loss represents the local mean of the channel gain and is therefore dependent on the distance between the transmitter and receiver. It also depends on the propagation environment. A path loss model is important for determination of the base station (cell) coverage area. Various path loss models have been proposed, mainly based on field measurements [106, 60, 81]. In this section, we study a few popular path loss models. To illustrate the distance-dependence of the propagation loss, we start with the propagation in free space.

#### 2.4.1 Free Space Propagation Model

When the distance between the transmitting antenna and receiving antenna is much larger than the wavelength of the transmitted wave and the largest physical linear dimension of the antennas, the power  $P_r$  at the output of the receiving antenna is given by [122]

$$P_r = P_t G_t G_r \left( \frac{\lambda}{4\pi d} \right)^2,$$

where

$P_t$  = total power radiated by an isotropic source,

$G_t$  = transmitting antenna gain,

$G_r$  = receiving antenna gain,

$d$  = distance between transmitting and receiving antennas,

$\lambda$  = wavelength of the carrier signal =  $c/f_c$ ,

$c$  =  $3 \times 10^8$  m/s (velocity of light),

$f_c$  = carrier frequency, and

$P_t G_t \stackrel{\Delta}{=} \text{effective isotropically radiated power (EIRP)}$ .

The term  $(4\pi d/\lambda)^2$  is known as the *free-space path loss* denoted by  $L_p(d)$ , which is

$$\begin{aligned} L_p(d) &= \frac{\text{EIRP} \times \text{Receiving antenna gain}}{\text{Received power}} \\ &= -10 \log_{10} \left[ \frac{\lambda^2}{(4\pi d)^2} \right] \text{ (dB)} \\ &= -20 \log_{10} \left( \frac{c/f_c}{4\pi d} \right) \text{ (dB)}. \end{aligned}$$

In other words, the path loss is

$$L_p(d) = 20 \log_{10} f_c + 20 \log_{10} d - 147.56 \text{ (dB).} \quad (2.4.3)$$

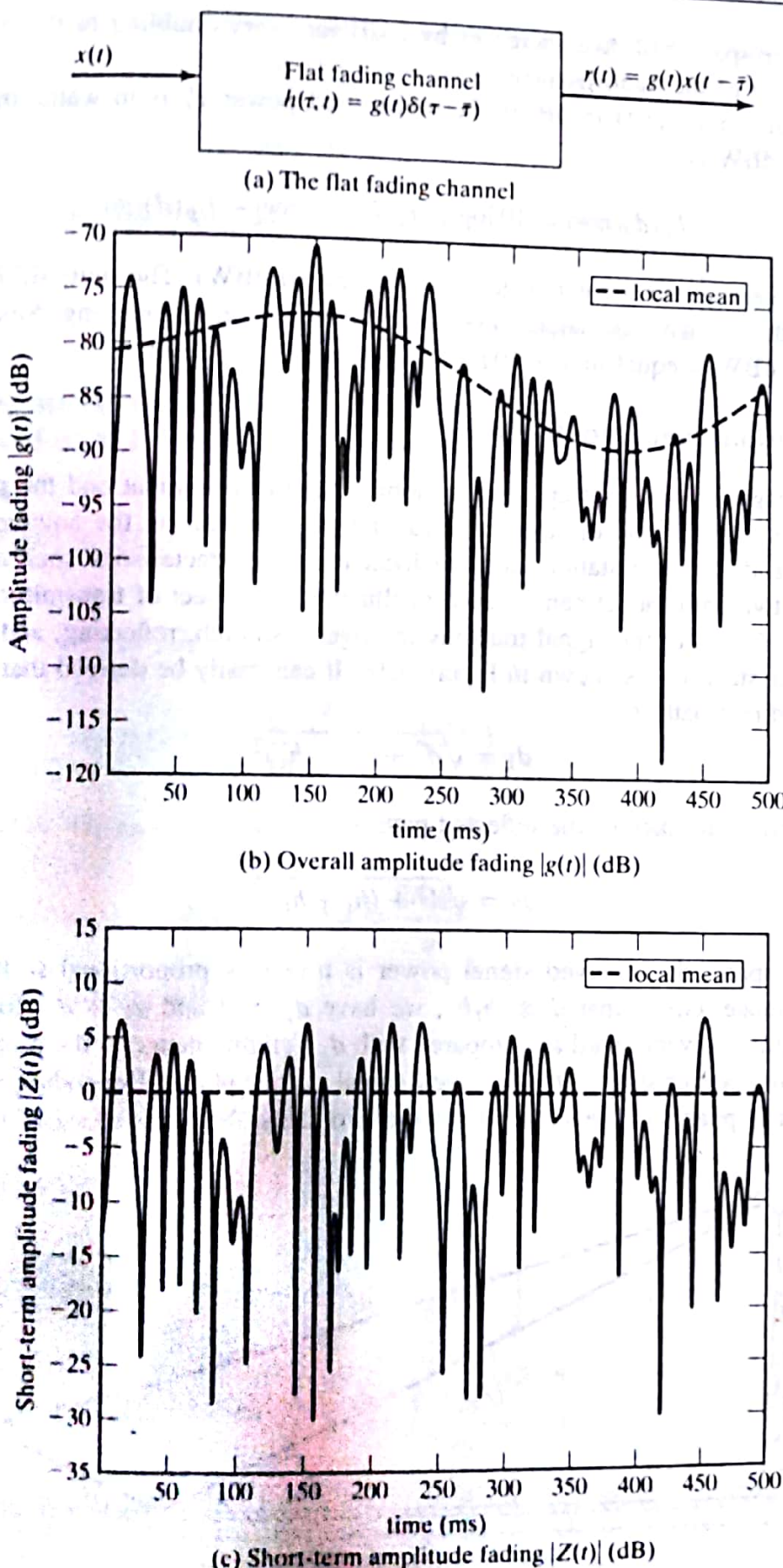


Figure 2.15 Representation of long-term and short-term fading components.

Note that the free-space path loss increases by 6 dB for every doubling of the distance and also for every doubling of the radio frequency.

With the path loss  $L_p(d)$  in dB, if the transmitted power  $P_t$  is in watts, then the received signal power in dBW is

$$P_r(d)_{(\text{dBW})} = 10 \log_{10}(P_t G_t G_r)_{(\text{dBW})} - L_p(d)_{(\text{dB})}. \quad (2.4.4)$$

The term dBW denotes dB greater or less than 1 watt (0 dBW). The units dBW and dBm (dB greater or less than 1 mW) are widely used in communication engineering. Since 1 W is equal to 1000 mW,  $x$  dBW is equal to  $x + 10 \log_{10} 1000 (= x + 30)$  dBm.

## 2.4.2 Propagation Over Smooth Plane

Free space propagation does not apply in a mobile radio environment and the propagation path loss depends not only on the distance and wavelength, but also on the antenna heights of the mobile station and the base station, and the local terrain characteristics such as buildings and hills. A simple two-path model can be used to illustrate the effect of transmitting and receiving antenna heights. Consider the signal transmission over a smooth, reflecting, and flat plane (such as earth or water surface), as shown in Figure 2.16. It can easily be derived that the propagation distance of the direct path is

$$d_1 = \sqrt{d^2 + (h_t - h_r)^2} \quad (2.4.5)$$

and the propagation distance of the reflected path is

$$d_2 = \sqrt{d^2 + (h_t + h_r)^2}. \quad (2.4.6)$$

In the free space, the received signal power is inversely proportional to the square of the propagation distance. Given that  $d \gg h_t, h_r$ , we have  $d_1 \approx d$  and  $d_2 \approx d$ . However, since the carrier wavelength  $\lambda$  is very small as compared with  $d$ , a slight change in the propagation distance can cause a significant change in the received signal carrier phase. Depending on the difference between the carrier phases of the signals from the two paths, the received signal components from

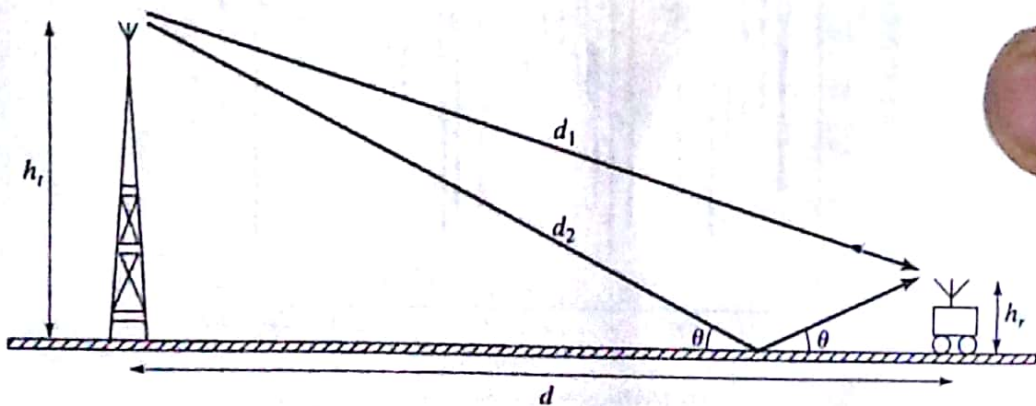


Figure 2.16 Two-path propagation over a flat plane.

the two paths may enhance each other or cancel each other. The carrier phase difference is related to the difference between the two propagation distances  $d_2$  and  $d_1$  by

$$\phi_2 - \phi_1 = \frac{2\pi}{\lambda} (d_2 - d_1). \quad (2.4.7)$$

Taking into account the phase difference, the received signal power is

$$P_r(d) = P_t G_t G_r \left( \frac{\lambda}{4\pi d} \right)^2 |1 + \alpha_f e^{-j\beta_f} \exp[j(\phi_2 - \phi_1)]|^2, \quad (2.4.8)$$

where  $\alpha_f$  and  $\beta_f$  are the amplitude attenuation and carrier phase shift, respectively, introduced by the reflection. If  $\alpha_f \approx 1$  (i.e., the reflection loss is negligible) and  $\beta_f = \pi$  for  $\theta \ll 1$ , then

$$\begin{aligned} P_r(d) &= P_t G_t G_r \left( \frac{\lambda}{4\pi d} \right)^2 \left| 1 - \cos\left(\frac{2\pi \Delta d}{\lambda}\right) - j \sin\left(\frac{2\pi \Delta d}{\lambda}\right) \right|^2 \\ &= P_t G_t G_r \left( \frac{\lambda}{4\pi d} \right)^2 \left[ 2 - 2 \cos\left(\frac{2\pi \Delta d}{\lambda}\right) \right] \\ &= 4 P_t G_t G_r \left( \frac{\lambda}{4\pi d} \right)^2 \sin^2\left(\frac{\pi \Delta d}{\lambda}\right), \end{aligned} \quad (2.4.9)$$

where  $\Delta d = d_2 - d_1$ . Given that  $d \gg h_t$  and  $d \gg h_r$ , from Eqs. (2.4.5)–(2.4.6), it can be derived that

$$\Delta d \approx \frac{2h_t h_r}{d}. \quad (2.4.10)$$

As a result, the received signal power is

$$P_r(d) \approx 4 P_t G_t G_r \left( \frac{\lambda}{4\pi d} \right)^2 \sin^2\left(\frac{2\pi h_t h_r}{\lambda d}\right). \quad (2.4.11)$$

The corresponding path loss is

$$\begin{aligned} L_p(d) &= \left[ 4 \left( \frac{\lambda}{4\pi d} \right)^2 \sin^2\left(\frac{2\pi h_t h_r}{\lambda d}\right) \right]^{-1} \\ &= -10 \log_{10} \left[ 4 \left( \frac{\lambda}{4\pi d} \right)^2 \sin^2\left(\frac{2\pi h_t h_r}{\lambda d}\right) \right] \text{ (dB)}. \end{aligned} \quad (2.4.12)$$

Figure 2.17 illustrates the path loss  $L_p(d)$  in dB as a function of the distance  $d$ , where  $f_c = 900$  MHz,  $h_t = 35$  m, and  $h_r = 3$  m. It is observed that (1) the path loss has alternate minima and maxima as the distance between the transmitter and receiver increases, and (2) in general, the path loss increases with the distance  $d$ .

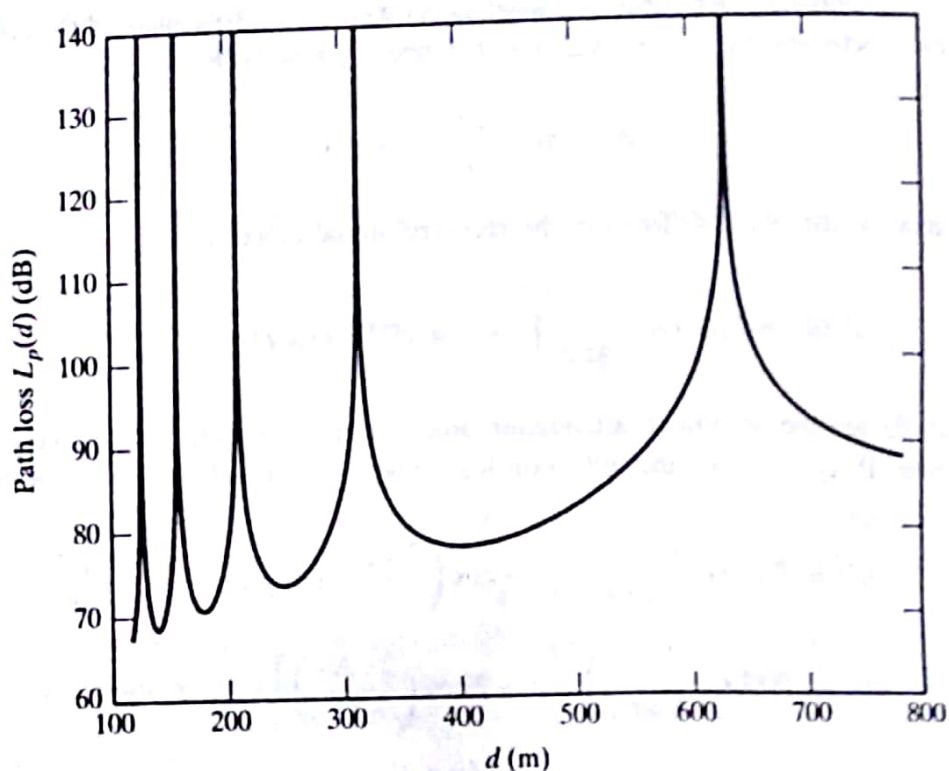


**Figure 2.17** The path loss  $L_p(d)$  in dB versus distance  $d$  in the two-path model.

### 2.4.3 Log-Distance Path Loss with Shadowing

As a mobile user moves away from its base station, the received signal becomes weaker because of the growing propagation attenuation with the distance. Let  $\bar{L}_p(d)$  denote the log-distance path loss, which is a function of the distance  $d$  separating the transmitter and the receiver. Then,

$$\bar{L}_p(d) \propto \left(\frac{d}{d_0}\right)^\kappa, \quad d \geq d_0$$

or equivalently,

$$\bar{L}_p(d) = \bar{L}_p(d_0) + 10\kappa \log_{10} \left( \frac{d}{d_0} \right) \text{ dB}, \quad d \geq d_0 \quad (2.4.13)$$

where  $\kappa$  is the path loss exponent and  $d_0$  is the close-in reference distance. Typically,  $d_0$  is 1 km for macrocells, 100 m for outdoor microcells, and 1 m for indoor picocells. Given  $d_0$ , the value  $\bar{L}_p(d_0)$  depends on the carrier frequency, antenna heights and gains, and other factors. Table 2.1 gives typical values of the path loss exponent in different propagation environments.

Furthermore, as the mobile moves in uneven terrain, it often travels into a propagation shadow behind a building or a hill or other obstacle much larger than the wavelength of the transmitted signal, and the associated received signal level is attenuated significantly. This phenomenon is called shadowing. A log-normal distribution is a popular model for characterizing the shadowing

**Table 2.1** Path Loss Exponents for Different Environments

Environment	Path Loss Exponent, $\kappa$
free space	2
urban cellular radio	2.7 to 3.5
shadowed urban cellular radio	3 to 5
in building with line of sight	1.6 to 1.8
obstructed in building	4 to 6

process. As a result, long-term fading is a combination of log-distance path loss and log-normal shadowing. Let  $\epsilon_{(dB)}$  be a zero-mean Gaussian distributed random variable (in dB) with standard deviation  $\sigma_\epsilon$  (in dB). The pdf of  $\epsilon_{(dB)}$  is given by

$$f_{\epsilon(dB)}(x) = \frac{1}{\sqrt{2\pi}\sigma_\epsilon} \exp\left(-\frac{x^2}{2\sigma_\epsilon^2}\right). \quad (2.4.14)$$

Let  $L_p(d)$  denote the overall path loss with shadowing (long-term fading) in dB. Then,

$$\begin{aligned} L_p(d) &= \bar{L}_p(d) + \epsilon_{(dB)} \\ &= \bar{L}_p(d_0) + 10\kappa \log_{10}\left(\frac{d}{d_0}\right) + \epsilon_{(dB)} \text{ (dB), } d \geq d_0. \end{aligned} \quad (2.4.15)$$

Since  $\epsilon_{(dB)}$  follows the Gaussian (normal) distribution with pdf given by Eq. (2.4.14),  $\epsilon$  in linear scale is said to follow a log-normal distribution with pdf given by

$$f_\epsilon(y) = \frac{20/\ln 10}{\sqrt{2\pi}y\sigma_\epsilon} \exp\left[-\frac{(20\log_{10}y)^2}{2\sigma_\epsilon^2}\right]. \quad (2.4.16)$$

The first-order statistics of log-normal shadowing are characterized by the standard deviation  $\sigma_\epsilon$ , which can be obtained from measurements. For example, 8 dB is a typical value for  $\sigma_\epsilon$  in an outdoor cellular system and 5 dB is a value for an indoor environment.

#### 2.4.4 Okumura–Hara Path Loss Model

The Okumura–Hara path loss model [106, 60] was developed by curve fitting the measurement data collected in Tokyo, Japan. It is suitable for outdoor macrocells. The path loss is represented as a function of (a) the carrier frequency  $f_c \in [150, 1000]$  MHz, (b) antenna heights of base station,  $h_b \in [30, 200]$  m, and mobile station,  $h_m \in [1, 10]$  m, and (c) the distance between the base station and mobile station  $d \in [1, 20]$  km. The path loss in dB is given by

$$L_p(d) = \begin{cases} A + B \log_{10}(d) & \text{for urban area} \\ A + B \log_{10}(d) - C & \text{for suburban area,} \\ A + B \log_{10}(d) - D & \text{for open area} \end{cases} \quad (2.4.17)$$

where

$$A = 69.55 + 26.16 \log_{10}(f_c) - 13.82 \log_{10}(h_b) - a(h_m),$$

$$B = 44.9 - 6.55 \log_{10}(h_b),$$

$$C = 5.4 + 2[\log_{10}(f_c/28)]^2,$$

$$D = 40.94 + 4.78[\log_{10}(f_c)]^2 - 18.33 \log_{10}(f_c),$$

and  $a(h_m)$  is the correction factor for mobile antenna height, and is given by

$$a(h_m) = [1.1 \log_{10}(f_c) - 0.7]h_m - [1.56 \log_{10}(f_c) - 0.8]$$

for a small to medium city and

$$a(h_m) = \begin{cases} 8.29[\log_{10}(1.54h_m)]^2 - 1.1 & \text{for } f_c \leq 200 \text{ MHz} \\ 3.2[\log_{10}(11.75h_m)]^2 - 4.97 & \text{for } f_c \geq 400 \text{ MHz} \end{cases}$$

for a large city.

Figure 2.18 shows the Okumura-Hara path loss in large city, suburban and open areas respectively as a function of  $d$  in km, with parameters  $f_c = 900$  MHz,  $h_b = 50$  m, and  $h_m = 3$  m.

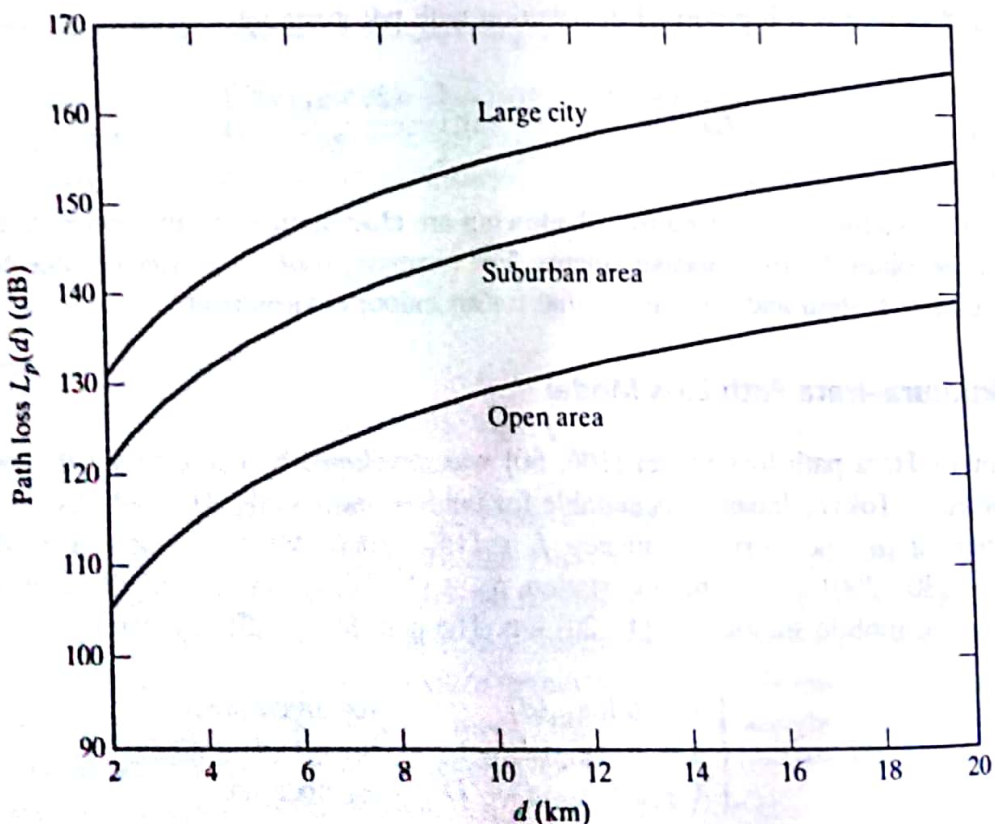


Figure 2.18 Propagation path loss using Okumura-Hara model.

### 2.4.5 Lee's Path Loss Model

Lee's model [81] can be used to predict area-to-area path loss. The model consists of two parts: (a) path loss prediction for a specified set of conditions, and (b) adjustment factors for a set of conditions different from the specified one. The model requires two parameters: (a) the power at a 1.6 km (1 mile) of interception  $P_0$  in dBm, and (b) the path-loss exponent  $\kappa$ . The specified set of conditions is as follows:

Carrier frequency  $f_c = 900$  MHz

Base station antenna height = 30.48 m (100 ft)

Base station power at the antenna = 10 W

Base station antenna gain = 6 dB above dipole gain

Mobile station antenna height = 3 m (10 ft)

Mobile station antenna gain = 0 dB above dipole gain

The received signal power in dBm is represented by

$$P_r(d) = P_{0(\text{dBm})} - 10\kappa \log_{10}(d/d_0) - 10n \log_{10}(f/f_c) + a_{0(\text{dB})}, \quad (2.4.18)$$

where  $d_0 = 1.6$  km,  $d$  ( $\geq d_0$ ) is the distance between the mobile station and the base station in km, and  $n$  is a constant between 2 and 3 dependent on the geographical locations and the operating frequency ranges.  $n = 2$  is recommended for a suburban or open area with  $f < 450$  MHz and  $n = 3$  for an urban area with  $f > 450$  MHz. The parameter  $a_{0(\text{dB})}$  is an adjustment factor for a different set of conditions

$$a_{0(\text{dB})} = 10 \log_{10}(a_1 a_2 a_3 a_4 a_5), \quad (2.4.19)$$

where

$$a_1 = \left[ \frac{\text{new base station antenna height (m)}}{30.48 \text{ (m)}} \right]^2$$

$$a_2 = \left[ \frac{\text{new mobile station antenna height (m)}}{3 \text{ (m)}} \right]^\nu$$

$$a_3 = \frac{\text{new transmitter power (W)}}{10 \text{ (W)}}$$

$$a_4 = \frac{\text{new base station antenna gain with respect to } \lambda/2 \text{ dipole}}{4}$$

$a_5$  = different antenna gain correction factor at the mobile station

The value  $\nu$  in  $a_2$  is obtained from empirical data and is given by

$$\nu = \begin{cases} 2 & \text{for new mobile station antenna height} > 10 \text{ m} \\ 1 & \text{for new mobile station antenna height} < 3 \text{ m} \end{cases}$$

**Table 2.2** The Parameters in Lee's Path Loss Model in Various Propagation Environments

terrain	$P_{0(\text{dBm})}$	$\kappa$
free space	-45	2.00
open area	-49	4.35
suburban areas	-61.7	3.84
urban area (Philadelphia)	-70	3.68
urban area (Newark)	-64	4.31
urban area (Tokyo)	-84	3.05

A 2 dB signal gain is provided by an actual 4 dB gain antenna at the mobile unit in a suburban area, and less than 1 dB gain received from the same antenna in an urban area for adjusting  $a_5$ . The two required parameters  $P_{0(\text{dBm})}$  and  $\kappa$  have been determined for various propagation environments based on empirical data and are given in Table 2.2.

The propagation path loss using Lee's model for some environments given in Table 2.2 is plotted in Figure 2.19, where the base station antenna height is 50 m with a gain of 6 dB with respect to a  $\lambda/2$  dipole, the transmitter power is 10 W, the mobile station antenna height is 3 m, and the carrier frequency  $f_c$  is 900 MHz.

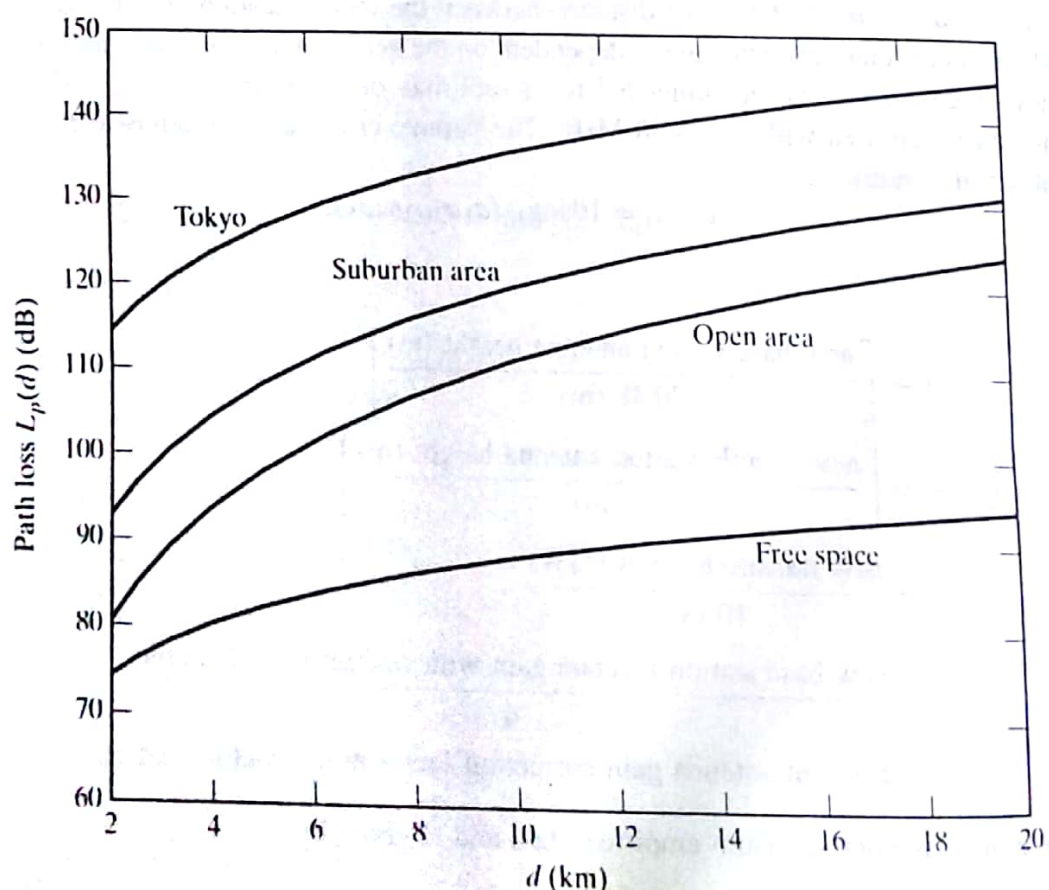


**Figure 2.19** Propagation path loss using Lee's model.

### 2.4.6 Radio Cell Coverage

Radio cell coverage is the service area supported by each base station. The coverage depends on (a) service quality requirements, such as the required ratio of the signal power to interference-plus-noise power (see Chapter 5 for more details), or the required minimum received signal power level given the transmitted signal power, and (b) the propagation environment. For example, for free space transmission with an omnidirectional antenna, the cell coverage is a circle centered at the base station (transmitter) with a radius depending on the propagation loss. Given the transmitted signal power level, the minimum required received power level can be mapped to the maximum allowed path loss. Then from Eq. (2.4.3), the cell radius ( $d$ ) can be determined. In practice, the path loss depends on the propagation environment, including the transmitter and receiver antenna heights, and may differ from angle to angle as seen from the base station transmitter antenna. As a result, the cell coverage will generally have an irregular shape (not a circle). Furthermore, because of the random nature in the path loss due to factors such as shadowing, the cell coverage is not deterministic but should be specified based on statistic parameters. The following example illustrates how to determine the cell coverage for a given propagation model, where the service quality criterion is specified in terms of the propagation path loss.

#### Example 2.5 Radio Cell Coverage for the Log-Distance Path Loss

Consider the log-distance path loss model. Determine the cell coverage for the following two situations:

- Without shadowing, the path loss is given by Eq. (2.4.13). It is required that, at the cell border, the path loss cannot be  $\gamma$  dB larger than that at the reference distance  $d_0$ .
- With shadowing, the path loss is given by Eq. (2.4.15). Due to the random nature of the propagation path loss, the cell coverage is defined as the service area of the base station over which the path loss (over that at the reference distance  $d_0$ ) is limited to  $\gamma$  dB with a pre-defined probability. Assume the reference distance  $d_0$  is very small compared with the cell radius.

#### Solution

- The path loss in dB at a distance  $d$  ( $> d_0$ ) from the base station is

$$\bar{L}_p(d) = \bar{L}_p(d_0) + 10\kappa \log_{10} \left( \frac{d}{d_0} \right).$$

As the path loss monotonically increases with the distance  $d$  and is independent of the propagation direction as observed at the base station, the cell coverage is a circle centered at the base station with radius  $R$  specified by

$$\Delta \bar{L}_p(d)|_{d=R} \triangleq \bar{L}_p(d)|_{d=R} - \bar{L}_p(d_0) = 10\kappa \log_{10} \left( \frac{d}{d_0} \right) \Big|_{d=R} \leq \gamma.$$

Solving the above equation for the radius  $R$ , we obtain

$$R \leq d_0 \times 10^{0.1(\gamma/\kappa)}.$$

- b. With shadowing, the path loss in dB at a distance  $d (> d_0)$  from the base station is

$$\bar{L}_p(d) = \bar{L}_p(d_0) + 10\kappa \log_{10} \left( \frac{d}{d_0} \right) + \epsilon_{(\text{dB})},$$

where the random variable  $\epsilon_{(\text{dB})}$  characterizes the effect of shadowing and is modeled by a Gaussian random variable with zero mean and standard deviation  $\sigma_\epsilon$  (in dB). The relative path loss at  $d (> d_0)$  with respect to the loss at  $d_0$  is given by

$$\Delta \bar{L}_p(d) \triangleq \bar{L}_p(d) - \bar{L}_p(d_0) = 10\kappa \log_{10} \left( \frac{d}{d_0} \right) + \epsilon_{(\text{dB})}.$$

The problem of estimating the cell coverage can be approached in two steps:

Step 1: Determine the probability  $a_1$  that the path loss at location  $r (> d_0)$  is below the threshold  $\gamma$ , where the probability is averaged over the circumference;

Step 2: Calculate the probability  $a_2$  of the circular area (defined by  $R$ ) over which the path loss is below the threshold based on  $a_1$ , where the probability is averaged over the circular area (cell area).

At the distance  $d = r (> d_0)$ , the probability that the relative path loss is limited to  $\gamma$  dB is

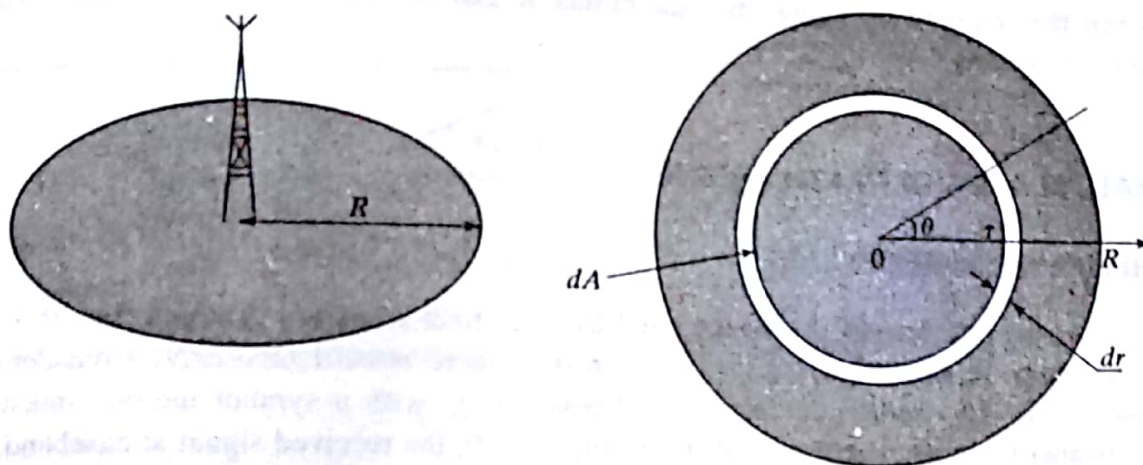
$$\begin{aligned} a_1(r) &= P(\Delta \bar{L}_p(r) \leq \gamma) \\ &= P(\epsilon_{(\text{dB})} \leq \gamma - 10\kappa \log_{10}(r/d_0)) \\ &= Q\left(\frac{\gamma - 10\kappa \log_{10}(r/d_0)}{\sigma_\epsilon}\right), \end{aligned} \quad (2.4.20)$$

where  $Q(x) \triangleq \frac{1}{\sqrt{2\pi}} \int_x^\infty \exp(-t^2/2) dt$ . Next, we want to find the probability  $a_2$  of the event " $\Delta \bar{L}_p(r) \leq \gamma$ " over a circular area  $A$  centered at the base station with radius  $R$ , as shown in Figure 2.20. The probability is given by

$$\begin{aligned} a_2 &= P(\Delta \bar{L}_p(r) \leq \gamma \text{ over the area } A) \\ &= \frac{1}{A} \int_A P(\Delta \bar{L}_p(r) \leq \gamma \text{ over the area } dA) dA \\ &= \frac{1}{A} \int_A a_1(r) dA, \end{aligned} \quad (2.4.21)$$

where  $A = \pi(R^2 - d_0^2) \approx \pi R^2$  for  $R \gg d_0$  and  $dA = rd\theta dr$  as shown in Figure 2.20. Substituting Eq. (2.4.20) into Eq. (2.4.21), we have

$$\begin{aligned} a_2 &\approx \frac{1}{\pi R^2} \int_0^{2\pi} d\theta \int_{d_0}^R a_1(r) r dr \\ &= 2 \int_{d_0/R}^R Q\left(\frac{\gamma - 10\kappa \log_{10}(r/d_0)}{\sigma_\epsilon}\right) \frac{r}{R} \frac{dr}{R} \\ &= 2 \int_{d_0/R}^1 Q\left(\frac{\gamma - 10\kappa \log_{10}(xR/d_0)}{\sigma_\epsilon}\right) x dx, \end{aligned}$$

**Figure 2.20** The cell coverage area.

where

$$\frac{\gamma - 10\kappa \log_{10}(xR/d_0)}{\sigma_\epsilon} = a - b \ln x,$$

with

$$a = \frac{\gamma - 10\kappa \log_{10}(R/d_0)}{\sigma_\epsilon}$$

and

$$b = \frac{10\kappa \log_{10} e}{\sigma_\epsilon}.$$

As a result,

$$\begin{aligned} a_2 &= 2 \int_{d_0/R}^1 \left[ \frac{1}{\sqrt{2\pi}} \int_{a-b \ln x}^{\infty} e^{-t^2/2} dt \right] x dx \\ &= 2 \left\{ \int_a^{a+b \ln(R/d_0)} \frac{1}{\sqrt{2\pi}} \left[ \int_{\exp(a-t/b)}^1 x dx \right] e^{-t^2/2} dt \right. \\ &\quad \left. + \int_{a+b \ln(R/d_0)}^{\infty} \frac{1}{\sqrt{2\pi}} \left[ \int_{d_0/R}^1 x dx \right] e^{-t^2/2} dt \right\} \\ &= Q(a) - \left( \frac{d_0}{R} \right)^2 Q \left( a + b \ln \left( \frac{R}{d_0} \right) \right) \\ &\quad - \exp \left( \frac{2ab+2}{b^2} \right) \left[ Q \left( a + \frac{2}{b} \right) - Q \left( a + \frac{2}{b} + b \ln \left( \frac{R}{d_0} \right) \right) \right]. \end{aligned}$$

If  $d_0 \ll R$ , we have

$$a_2 \approx Q(a) - \exp \left( \frac{2ab+2}{b^2} \right) \left[ Q \left( a + \frac{2}{b} \right) - Q \left( a + \frac{2}{b} + b \ln \left( \frac{R}{d_0} \right) \right) \right].$$

Given the required  $a_2$  value, the cell radius  $R$  can be determined numerically from the above equations.

## 2.5 SMALL-SCALE MULTIPATH FADING

### 2.5.1 First-Order Statistics

Suppose the multipath channel is characterized by  $N$  distinct scatterers in which the  $n$ th scatterer is associated with a gain  $\alpha_n(t)$  and a delay  $\tau_n(t)$ , where  $n = 1, 2, \dots, N$ . Consider digital transmission over the channel at the carrier frequency  $f_c$  with a symbol interval much larger than the channel multipath delay spread. From Eq. (2.2.2), the received signal at baseband, in the absence of background noise, is

$$\begin{aligned} r(t) &= \sum_{n=1}^N \alpha_n(t) e^{-j2\pi f_c \tau_n(t)} x(t - \tau_n(t)) \\ &\approx \left[ \sum_{n=1}^N \alpha_n(t) e^{-j2\pi f_c \tau_n(t)} \right] x(t - \bar{\tau}). \end{aligned}$$

The approximation is reasonable as long as the delay spread is much smaller than the symbol interval. The complex gain of the channel is  $Z(t) = \sum_{n=1}^N \alpha_n(t) e^{-j2\pi f_c \tau_n(t)}$ . Let  $Z_c(t)$  and  $-Z_s(t)$  denote the real and imaginary components of the complex channel gain, respectively, so that  $Z(t) = Z_c(t) - jZ_s(t)$ . Then

$$\begin{aligned} Z_c(t) &= \sum_{n=1}^N \alpha_n(t) \cos \theta_n(t) \\ Z_s(t) &= \sum_{n=1}^N \alpha_n(t) \sin \theta_n(t), \end{aligned}$$

where  $\theta_n(t) = 2\pi f_c \tau_n(t)$ .

Furthermore, let

$$\alpha(t) = \sqrt{Z_c^2(t) + Z_s^2(t)}, \quad \theta(t) = \tan^{-1}[Z_s(t)/Z_c(t)]$$

be the amplitude fading and carrier distortion introduced by the channel. The fading characteristics can be studied by examining the pdfs of the envelope  $\alpha(t)$  and phase  $\theta(t)$  at any time  $t$ . The fading characteristics depend on whether the transmitter and receiver are in line-of-sight or not in line-of-sight. The former case is called LOS scattering while the latter case is referred to as NLOS scattering. LOS scattering has a specular component (from the direct path), and can be modeled as a Rician distribution. NLOS scattering does not have a specular component, and can be modeled as a Rayleigh distribution. A pictorial view of LOS and NLOS scattering is depicted in Figure 2.21.

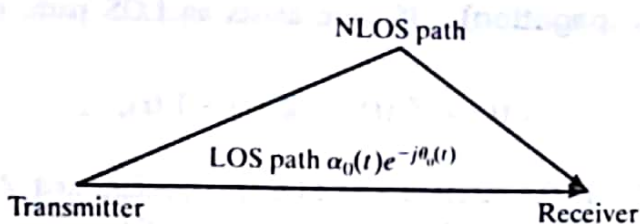


Figure 2.21 NLOS versus LOS scattering.

**Rayleigh Fading (NLOS propagation).** In this case,

$$E[Z_c(t)] = E[Z_s(t)] = 0. \quad (2.5.1)$$

Assume that, at any time  $t$ , for  $n = 1, 2, \dots, N$ ,

- a. the values of  $\theta_n(t)$  are statistically independent, each being uniformly distributed over  $[0, 2\pi]$ ;
- b. the values of  $\alpha_n(t)$  are identically distributed random variables, independent of each other and of the  $\theta_n(t)$ 's.

According to the central limit theorem,  $Z_c(t)$  and  $Z_s(t)$  are approximately Gaussian random variables at any time  $t$  if  $N$  is sufficiently large. For simplicity of notation, let  $Z_c$  and  $Z_s$  denote  $Z_c(t)$  and  $Z_s(t)$  at any time  $t$ . It can be shown that  $Z_c$  and  $Z_s$  are independent Gaussian random variables with zero mean and equal variance  $\sigma_z^2 = \frac{1}{2} \sum_{n=1}^N E[\alpha_n^2]$ , where  $\alpha_n$  denotes  $\alpha_n(t)$  at any time  $t$ . As a result, the joint pdf of  $Z_c$  and  $Z_s$  is

$$f_{Z_c Z_s}(x, y) = \frac{1}{2\pi\sigma_z^2} \exp\left[-\frac{x^2 + y^2}{2\sigma_z^2}\right], \quad -\infty < x < \infty, \quad -\infty < y < \infty. \quad (2.5.2)$$

Let  $\alpha$  and  $\theta$  be the amplitude fading  $\alpha(t)$  and carrier phase distortion  $\theta(t)$  at any time  $t$ . Then it can easily be shown that

- a. the amplitude fading,  $\alpha$ , follows a Rayleigh distribution with parameter  $\sigma_z^2$ ,

$$f_\alpha(x) = \begin{cases} \frac{x}{\sigma_z^2} \exp\left(-\frac{x^2}{2\sigma_z^2}\right), & x \geq 0 \\ 0, & x < 0 \end{cases}, \quad (2.5.3)$$

with  $E[\alpha] = \sigma_z \sqrt{\pi/2}$  and  $E(\alpha^2) = 2\sigma_z^2$ ;

- b. the phase distortion follows a uniform distribution over  $[0, 2\pi]$ ,

$$f_\theta(x) = \begin{cases} \frac{1}{2\pi}, & 0 \leq x \leq 2\pi \\ 0, & \text{elsewhere} \end{cases}; \quad (2.5.4)$$

- c. the amplitude fading  $\alpha$  and the phase distortion  $\theta$  are independent.

The channel is called a Rayleigh fading channel.

**Rician Fading (LOS propagation).** If there exists an LOS path, the channel gain can be represented by

$$Z(t) = Z_c(t) - jZ_s(t) + \Gamma(t),$$

where  $\Gamma(t) = \alpha_0(t)e^{-j\theta_0(t)}$  is the deterministic LOS component, and  $Z_c(t) - jZ_s(t)$  represents all the NLOS components. With the LOS component,  $E[Z(t)] = \Gamma(t) \neq 0$ . The distribution of the envelope at any time  $t$  is given by the Rayleigh distribution modified by

- a. a factor containing a non-centrality parameter, and
- b. a zero-order modified Bessel function of the first kind.

The resultant pdf for the amplitude fading at any  $t$ ,  $\alpha$ , is known as the Rician distribution, given by (see Appendix D)

$$\begin{aligned} f_\alpha(x) &= \underbrace{\frac{x}{\sigma_z^2} \exp\left(-\frac{x^2}{2\sigma_z^2}\right)}_{\text{Rayleigh}} \cdot \underbrace{\exp\left\{-\frac{\alpha_0^2}{2\sigma_z^2}\right\} \cdot I_0\left(\frac{\alpha_0 x}{\sigma_z^2}\right)}_{\text{modifier}} \\ &= \frac{x}{\sigma_z^2} \exp\left(-\frac{x^2 + \alpha_0^2}{2\sigma_z^2}\right) I_0\left(\frac{\alpha_0 x}{\sigma_z^2}\right), \quad x \geq 0, \end{aligned} \quad (2.5.5)$$

where  $\alpha_0$  is  $\alpha_0(t)$  at any  $t$ .  $\alpha_0^2$  is the power of the LOS component and is the non-centrality parameter,  $I_0(\cdot)$  is the zero-order modified Bessel function of the first kind and is given by

$$I_0(x) = \frac{1}{2\pi} \int_0^{2\pi} \exp(x \cos \theta) d\theta. \quad (2.5.6)$$

The Rician fading channel has an important parameter called the  $K$  factor. It is defined as

$$K \triangleq \frac{\text{Power of the LOS component}}{\text{Total power of all other scattered components}} = \frac{\alpha_0^2}{2\sigma_z^2}.$$

As  $K$  approaches zero, the Rician distribution approaches the Rayleigh distribution. On the other hand, as  $K$  approaches infinity, only the dominant component matters and there is no fading. As a result, the wireless channel approaches an AWGN channel. Figure 2.22 shows the Rician distribution with  $\sigma_z = 1$  and various  $K$  values. Assuming  $\theta_0(t) = \pi/2$ , it can be derived that, at a given  $t$ , the pdf of the carrier phase distortion  $\theta(t)$  is given by

$$f_\theta(x) = \frac{1}{2\pi} \exp(-K) + \frac{1}{2} \sqrt{\frac{K}{\pi}} (\cos x) \exp(-K \sin^2 x) [1 + \operatorname{erf}(\sqrt{K} \cos x)] \quad (2.5.7)$$

for  $x \in [-\pi, +\pi]$ , where  $\operatorname{erf}(x) = \frac{2}{\sqrt{\pi}} \int_0^x e^{-y^2} dy$  is the error function.

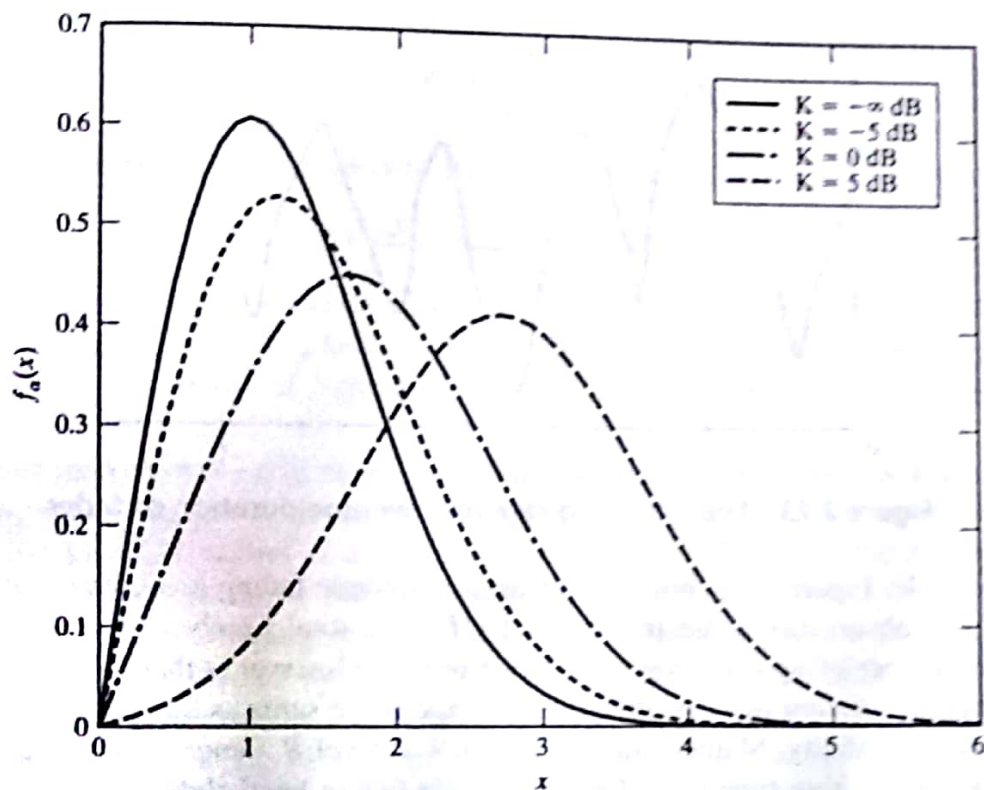


**Figure 2.22** Rayleigh and Rician fading distributions with  $\sigma_z = 1$ .

### 2.5.2 Second-Order Statistics

The pdfs of the amplitude fluctuation and phase distortion of a fading channel in Section 2.4 tell us how the amplitude and phase will behave at each time instant, but do not tell us how they change with time. In designing efficient modulation and channel coding schemes to combat channel fading, just knowing the pdfs of the amplitude fading and carrier phase distortion introduced by the channel is not enough. How fast channel fading changes with time is also important. Level crossing rate (LCR) and average fade duration (AFD) are two statistics which describe the frequency of fading. They are closely related to the Doppler frequency shifts introduced by the channel. Although the second-order statistics provide the same information as the channel correlation functions (in particular, the channel coherence time and Doppler spread) given in Section 2.3, LCR and AFD are defined more specifically and, therefore, their mathematical expressions can be derived for a flat Rayleigh fading channel. In the following discussion, we are interested in LCR and AFD for the short-term amplitude fading and, in particular, for a WSS and ergodic<sup>2</sup> Rayleigh flat fading channel.

#### Level Crossing Rate

**Definition 2.3** The crossing rate at level  $R$  of a flat fading channel is the expected number of times that the channel amplitude fading level,  $\alpha(t)$ , crosses the specified level  $R$ , with a positive slope, divided by the observation time interval.

<sup>2</sup>An ergodic process is one in which any state will occur with a non-zero probability; every sizable sample is equally representative of the whole.

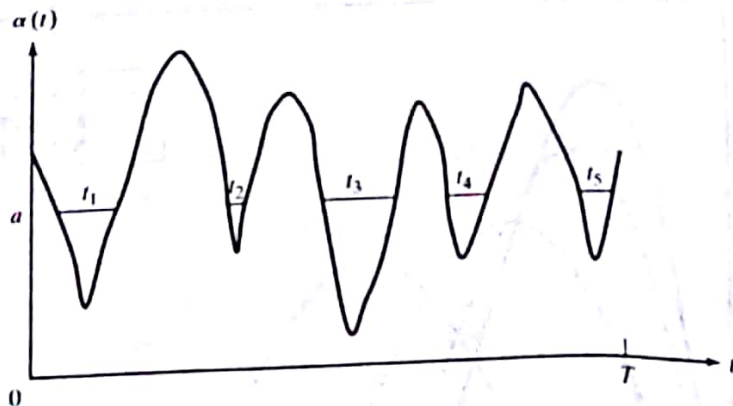


Figure 2.23 Level crossing rate and average duration of fades.

As an example, Figure 2.23 shows the channel amplitude fading level, where  $R$  is the chosen threshold. If the observation time interval is  $[0, T]$ , the total number of positive crossings is  $M_T = 5$ . The number of up crossings per second over the interval is then  $M_T/T = 5/T$ .

For an ergodic random process, statistical average is the same as time average when the time interval approaches infinity. Mathematically, the LCR at level  $R$ , denoted by  $N_R$ , is defined as the expectation of the positive time rate of the amplitude fading level change at the given threshold  $R$ . That is

$$N_R = E[\text{upward crossing rate at level } R]. \quad (2.5.8)$$

Let  $\dot{\alpha}$  denote the amplitude fading rate,  $d\alpha(t)/dt$ , at any time  $t$ , and let  $f_{\alpha\dot{\alpha}}(x, y)$  denote the joint pdf of the amplitude fading  $\alpha(t)$  and its derivative  $\dot{\alpha}(t)$  at any time  $t$ . Then  $f_{\alpha\dot{\alpha}}(x, y)|_{x=R}$  gives the joint pdf at the amplitude level  $R$ . From the definition, LCR is the expectation of the positive rate (i.e.,  $\dot{\alpha} > 0$ ) and at the level  $R$ , which can be expressed by

$$N_R = \int_0^\infty y f_{\alpha\dot{\alpha}}(x, y)|_{x=R} dy. \quad (2.5.9)$$

For the Rayleigh fading environment studied in Subsection 2.5.1, it can be shown that [130]

$$f_{\alpha\dot{\alpha}}(x, y) = \frac{x}{\sqrt{2\pi\sigma_\alpha^2\sigma_{\dot{\alpha}}^2}} \exp\left[-\frac{1}{2}\left(\frac{x^2}{\sigma_\alpha^2} + \frac{y^2}{\sigma_{\dot{\alpha}}^2}\right)\right], \quad x \geq 0, -\infty < y < \infty, \quad (2.5.10)$$

where

$$\sigma_{\dot{\alpha}}^2 = \frac{1}{2}(2\pi v_m)^2 \sigma_z^2$$

and  $v_m$  is the maximum Doppler shift. Substituting Eq. (2.5.10) into Eq. (2.5.9), the LCR is

$$\begin{aligned} N_R &= \int_0^\infty y \cdot \frac{R}{\sqrt{2\pi\sigma_\alpha^2\sigma_{\dot{\alpha}}^2}} \exp\left[-\frac{1}{2}\left(\frac{R^2}{\sigma_\alpha^2} + \frac{y^2}{\sigma_{\dot{\alpha}}^2}\right)\right] dy \\ &= \sqrt{2\pi} v_m \left(\frac{R}{\sqrt{2}\sigma_z}\right) \exp\left(-\frac{R^2}{2\sigma_z^2}\right). \end{aligned}$$

Letting

$$\rho = \frac{R}{\sqrt{2}\sigma_z}$$

be the normalized threshold with respect to the rms value of  $\alpha$  (i.e.,  $\sqrt{2}\sigma_z$ ), we have

$$N_R = \sqrt{2\pi} v_m \rho \exp(-\rho^2). \quad (2.5.11)$$

The LCR is a product of two terms. The first term,  $\sqrt{2\pi} v_m$ , is proportional to the maximum Doppler shift. Since  $v_m = \frac{V f_c}{c}$ , where  $V$  is the velocity of the mobile user,  $f_c$  is the carrier frequency, and  $c$  is the speed of light, LCR is proportional to the user speed and the carrier frequency.

The second term,  $\rho \exp(-\rho^2)$ , depends only on the normalized threshold. Figure 2.24 shows how the component changes with the normalized threshold  $\rho$  in dB. It is observed that the maximum value for LCR occurs at a value of  $\rho$  which is 3 dB below the rms value. This is always true and can be proved by differentiating Eq. (2.5.11) with respect to  $\rho$  and setting the result to zero. The sharp dropping of the LCR for values of  $\rho$  above the rms value, as shown in Figure 2.24, can be explained by Figure 2.25. Recall that the basic definition of LCR is the number of up crossings divided by the observation interval. In Figure 2.25, let the signal level  $c$  be the rms value. When the signal level moves from  $c$  to  $b$ , the number of crossings decreases rapidly. This is the reason why the LCR shown in Figure 2.24 drops so fast. Similarly, the LCR value decreases when the value of  $\rho$  is more than 3 dB smaller than the rms value, as can be

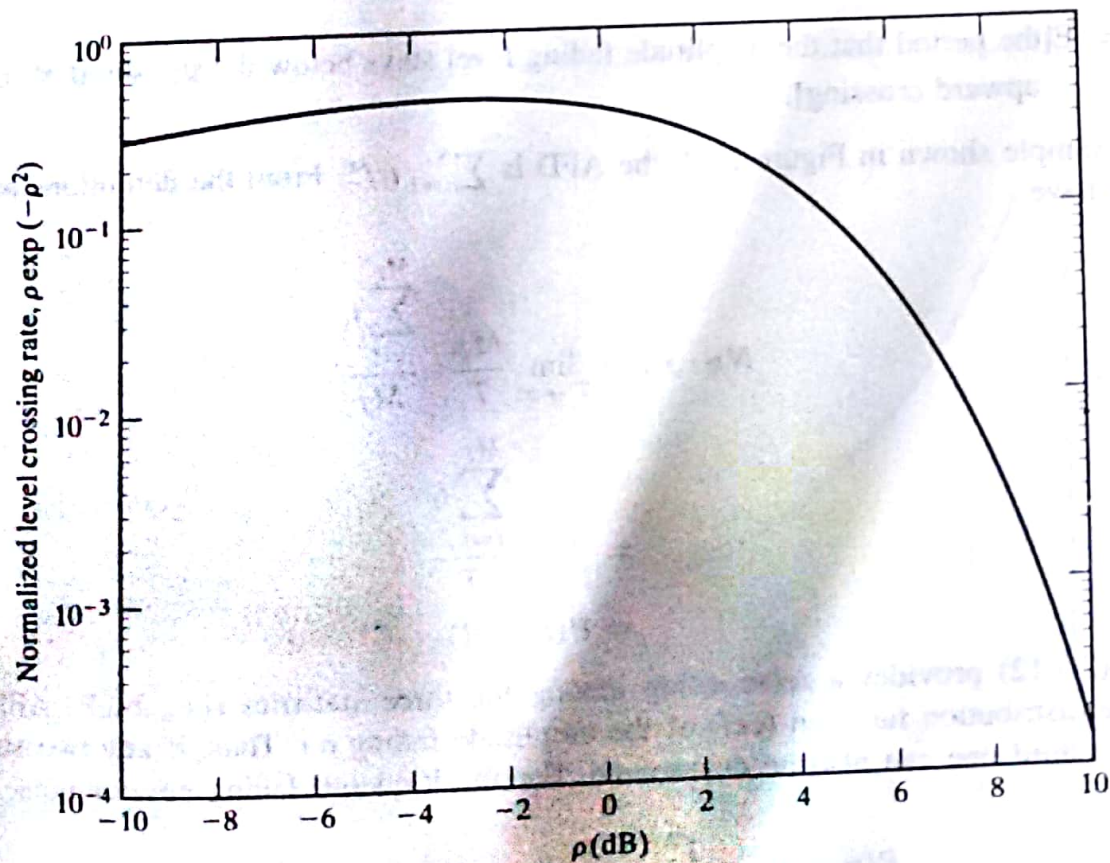
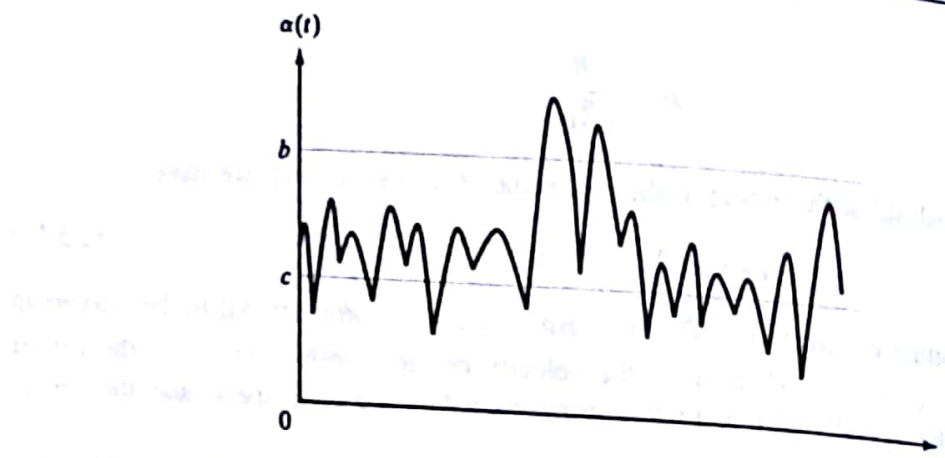


Figure 2.24 The normalized level crossing rate of the flat Rayleigh fading channel.



**Figure 2.25** An example of amplitude fading level versus time.

observed from Figure 2.24. The maximum LCR is achieved at  $\rho = -3$  dB, because the pdf of  $\alpha$  is maximized at the threshold.

### Average Fade Duration

**Definition 2.4** The average fade duration at level  $R$  is the average period of time for which the channel amplitude fading level is below the specified threshold  $R$  during each fade period.

Let  $\chi_R$  denote the AFD. It is a statistic closely related to the LCR. Mathematically, the AFD

$$\chi_R = E[\text{the period that the amplitude fading level stays below the threshold } R \text{ in each upward crossing}].$$

For the example shown in Figure 2.23, the AFD is  $\sum_{i=1}^5 t_i / 5$ . From the definitions of LCR and AFD, we have

$$\begin{aligned} N_R \cdot \chi_R &= \lim_{T \rightarrow \infty} \frac{M_T}{T} \cdot \frac{\sum_{i=1}^{M_T} t_i}{M_T} \\ &= \lim_{T \rightarrow \infty} \frac{\sum_{i=1}^{M_T} t_i}{T} \\ &= P(\alpha \leq R). \end{aligned} \quad (2.5.12)$$

Equation (2.5.12) provides a relationship among the three statistics (i.e., LCR, AFD, and the cumulative distribution function (cdf) of the amplitude fading  $\alpha$ ). Thus, if any two statistics are known, the third one can also be determined. For the Rayleigh fading environment, the cdf of  $\alpha$  is

$$P(\alpha \leq x) = \int_0^x f_\alpha(y) dy = 1 - \exp\left(-\frac{x^2}{2\sigma_z^2}\right). \quad (2.5.13)$$

By Eqs. (2.5.11)–(2.5.13), the corresponding AFD is

$$\begin{aligned}\chi_R &= \frac{P(A \leq R)}{N_R} \\ &= \frac{1 - \exp(-R^2/2\sigma_z^2)}{\sqrt{2\pi} v_m (R/\sqrt{2\sigma_z^2}) \exp(-R^2/2\sigma_z^2)} \\ &= \frac{\exp(\rho^2) - 1}{\sqrt{2\pi} v_m \rho}.\end{aligned}\quad (2.5.14)$$

The AFD is a product of two components. The first component,  $1/(\sqrt{2\pi} v_m)$ , indicates that the AFD is inversely proportional to the mobile speed and the carrier frequency.

The second term,  $[\exp(\rho^2) - 1]/\rho$ , depends only on the normalized threshold  $\rho$ . Figure 2.26 shows how the component changes with the normalized threshold in dB. The value of the AFD increases dramatically as the threshold  $\rho$  increases much above the rms value. This can be explained from Figure 2.25. With a large threshold value, it is very unlikely for the amplitude level  $\alpha$  to cross the threshold. Therefore, the length of time that  $\alpha$  stays below the threshold can be very long.

Knowledge of the AFD value helps to determine the most likely number of bits that may be lost during a fade. This is useful for relating the received signal-to-noise ratio (SNR) during a fade to the instantaneous bit error rate (BER).

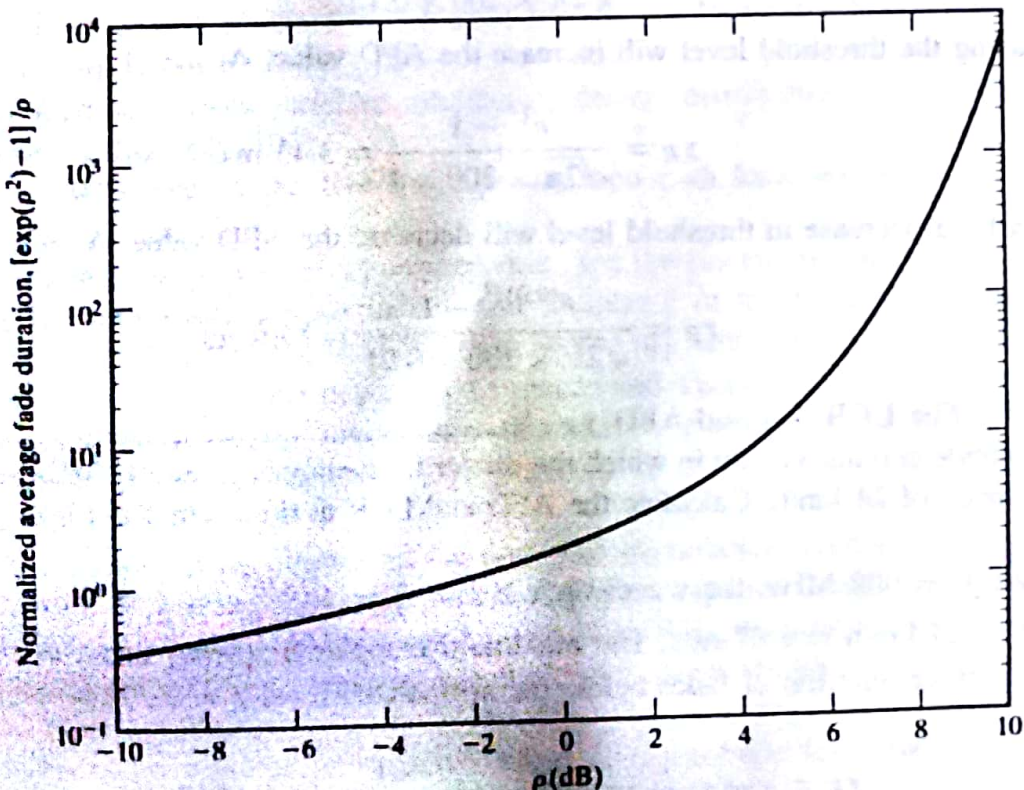


Figure 2.26 The normalized average fade duration of the flat Rayleigh fading channel.

**Example 2.6 The LCR  $N_R$** 

Consider a flat Rayleigh fading channel. Determine the positive-going level crossing rate for  $\rho = 1$ , when the maximum Doppler frequency  $v_m = 20$  Hz. Compute the maximum velocity of the mobile if the carrier frequency is 900 MHz.

**Solution**

$$\begin{aligned} N_R &= \sqrt{2\pi} v_m \rho e^{-\rho^2}; \quad v_m = 20 \text{ Hz}, \quad \rho = 1 \\ &= \sqrt{2\pi} \times 20 \times 1 \times e^{-1} \\ &= 18.44 \text{ crossings per second.} \end{aligned}$$

The maximum velocity is  $V_m = v_m \cdot \frac{c}{f_c} = 20 \times \frac{3 \times 10^8}{9 \times 10^8} \text{ m/s} = 6.66 \text{ m/s} = 24 \text{ km/hr.}$

**Example 2.7 The AFD  $\chi_R$** 

Suppose a flat Rayleigh fading channel exhibits a maximum Doppler frequency  $v_m = 200$  Hz.

- Determine the average fade duration for a normalized threshold level  $\rho = 0.1$ .
- How does the result in part (a) changes when  $\rho$  is increased to 1.0?
- How does the result in part (a) changes when  $\rho$  is reduced to 0.01?

**Solution**

- a. At  $\rho = 0.1$ ,

$$\chi_R = \frac{e^{(0.1)^2} - 1}{\sqrt{2\pi} \times 200 \times 0.1} = 200 \mu\text{s.}$$

- b. Increasing the threshold level will increase the AFD value. At  $\rho = 1$ ,

$$\chi_R = \frac{e^{1^2} - 1}{\sqrt{2\pi} \times 200 \times 1} = 3.43 \text{ ms.}$$

- c. Similarly, a decrease in threshold level will decrease the AFD value. At  $\rho = 0.01$ ,

$$\chi_R = \frac{e^{(0.01)^2} - 1}{\sqrt{2\pi} \times 200 \times 0.01} = 19.9 \mu\text{s.}$$

**Example 2.8 The LCR  $N_R$  and AFD  $\chi_R$** 

Consider a mobile cellular system in which the carrier frequency is  $f_c = 900$  MHz and the mobile travels at a speed of 24 km/h. Calculate the AFD and LCR at the normalized level  $\rho = 0.294$ .

**Solution** At  $f_c = 900$  MHz, the wavelength is  $\lambda = \frac{c}{f_c} = \frac{3 \times 10^8}{900 \times 10^6} = \frac{1}{3}$  m. The velocity of the mobile is  $V = 24 \text{ km/h} = 6.67 \text{ m/s}$ . The maximum Doppler frequency is  $v_m = V/\lambda = \frac{6.67}{1/3} = 20 \text{ Hz}$ . The average duration of fades below the normalized level  $\rho = 0.294$  is

$$\chi_R = \frac{e^{\rho^2} - 1}{\sqrt{2\pi} v_m \rho} = \frac{e^{(0.294)^2} - 1}{\sqrt{2\pi} \times 20 \times 0.294} = 0.0061 \text{ s.}$$

The level crossing rate at  $\rho = 0.294$  is

$$\begin{aligned}N_R &= \sqrt{2\pi} v_m \rho e^{-\rho^2} \\&= \sqrt{2\pi} \times 20 \times 0.294 e^{-(0.294)^2} \\&= 16 \text{ upcrossings/second.}\end{aligned}$$

## SUMMARY

Unlike a guided wire, the wireless propagation channel is prone to atmospheric conditions. A consequence of this is that electromagnetic propagation through the wireless channel will suffer different degrees of impairment. To understand the channel disturbance on the transmitted signal, so as to facilitate transmitter and receiver design as a means of combating channel impairments, we have examined commonly used analytical methods for modeling the channel characteristics. The next chapter will study modulation methods commonly used in a mobile radio environment.

## ENDNOTES

1. For a general discussion on channel fading and its characterization, see the paper by Sklar [140] and the book by Kennedy [71].
2. For detailed discussion of the LTV channel model, the channel functions, and correlation functions, see the paper by Bello [12].
3. For background on random variables, probability density distributions, and random processes, see the book by Papoulis [108].
4. For detailed derivation of the free-space propagation path loss, see the book by Pratt and Bostian [122].
5. For path loss models in an outdoor environment, see the papers by Okumura *et al.* [106] and Hata [60] for the Okumura-Hata model, and Chapter 2 of the book by Lee [81] for Lee's model. Other models are given in [129], [89], [43], [36], and [156].
6. For cell coverage area, see the papers by Leonardo and Yacoub [83, 84].
7. Characterization of an indoor propagation channel is reviewed in the paper by Hashemin [59]. A statistical model for indoor propagation is given in the paper by Saleh and Valenzula [133].
8. For detailed analysis of the short-term flat fading characteristics (such as Rayleigh and Rician fading), see the papers by Clarke [30] and Lee [78], Chapter 1 of the book edited by Jakes [42], and Chapters 3 and 4 of the book by Lee [82]. For computer simulation of correlated Rayleigh and Rician fading channels, see the book edited by Jakes [42] and the paper by Young and Beaulieu [162].
9. Other references on wireless propagation channels include the textbooks by Griffiths [56], Parsons [109], and Rappaport [128].